INVESTIGATION OF A PROPOSED TECHNIQUE FOR MEASUREMENTS OF DIELECTRIC CONSTANTS AND LOSSES AT V-BAND USING THE FABRY-PEROT PRINCIPLE

A Thesis

Presented to

the Faculty of the School of Engineering and Applied Science

University of Virginia

In Partial Fulfillment

of the Requirements for the Degree

Master of Electrical Engineering

by

Constantine A. Balanis

August 1966

APPROVAL SHEET

This thesis is submitted in partial fulfillment of

the requirements for the degree of

Master of Electrical Engineering

_____

Author

Approved:

_____

Faculty Adviser

_____

Dean, School of Engineering
and Applied Science

June 30, 1966

ACKNOWLEDGEMENTS

The author wishes to acknowledge Doctors Foster and Harris for their helpful suggestions and criticisms, Mr. W. F. Cuddihy of the Telemeter Techniques Research Section and the NASA Langley Research Center for permitting this work to be submitted as a thesis.

TABLE OF CONTENTS

LIST OF TABLES

LIST OF FIGURES

FIGURE PAGE

LIST OF SYMBOLS

A	surface area of reflector plate
A_i, B_j	amplitudes of electric and magnetic fields
^oC	degrees—centigrade
E	electric field intensity
GHz	gigahertz $(10^9$ cycles per second$)$
H	magnetic field intensity
L	focal length
MHz	megahertz $(10^6$ cycles per second$)$
P	polarization
P_d	diffraction losses
P_s	dissipated power in the cavity
Q_o	quality factor of the cavity without the dielectric sheet
Q_t	quality factor of the cavity with the dielectric sheet
R	radius of curvature
R_s	real part of the surface impedance of the plates
V	volume of the cavity
W_s	stored energy in the cavity
Z	impedance
a,b	distances between centers of coupling holes in Y and Z directions, respectively
d	plate separation
dB	decibel
f	frequency
Δf	half-power bandwidth of cavity response

k	index of refraction
n	a constant
r	radius of coupling holes
s_1	slab thickness
s_2, s_3	relative distances between dielectric sheet and plate no. 2
t	transmission coefficient
w	angular frequency
Δ	shift of plate no. 2 necessary to restore resonance
α	attenuation constant
β	phase constant
γ	reflection and diffraction losses
ϵ	dielectric constant
μ	permeability constant
ρ	reflection coefficient
τ	relaxation time
$\tan\delta$	loss tangent

ABSTRACT 32299

The difficulties existing in applying methods consistently used for the measurements of dielectric constants and losses in lower microwave frequencies at millemeter waves are presented. A method using a Fabry-Perot interferometer as a resonant cavity for the measurements of dielectric constants and losses in the millimeter region is discussed. The advantages of using such a system are that its physical dimensions are many times larger than the operating wavelength and a relative high Q can be obtained thus providing a system of high sensitivity in the measurements of dielectric constants and losses. Experimental data of dielectric constants and losses for teflon, polystyrene and plexiglas are presented at approximately 60 GHz. Samples of several thicknesses and various surface finishes were used and the results compared. Also, comparison with data at lower microwave frequencies was made. Values of dielectric constants in a small frequency band were measured at constant temperature. To determine the effect of temperature on the dielectric properties at millimeter waves, the dielectric constant was measured at different temperatures.

CHAPTER I

INTRODUCTION

The dielectric constants and loss tangents of dielectric materials depend upon the frequency of the applied electric field. The calculation of the permittivity of dielectrics is usually very difficult, because it depends on the lattice structure of the medium. The dielectric constant of a material is a function of its polarization. A plot of the real part of the polarization as a function of frequency[1] is shown in Figure 1. The polarization is shown to be constant for frequencies up to, but not including, the microwave region. In the microwave region, a decrease in polarization occurs. This is due to the damping of the dipolar polarization behind the applied electric field which eventually reaches zero. Between microwave and infrared frequencies, a region of constant polarization occurs and is equal to the atomic and electronic polarization. Another transition in polarization occurs through the infrared region and is due to the change in the atomic polarization. Between the infrared and ultraviolet region, constant polarization exists and is equal to the electronic polarization. In the ultraviolet region another transition occurs, and this is due to the variation in the electronic polarization. The permittivity of some dielectrics can be approximated by the simulation

---

[1] A.J. Decker, Solid State Physics (New York: Prentice Hall, Inc., 1946), p. 157.

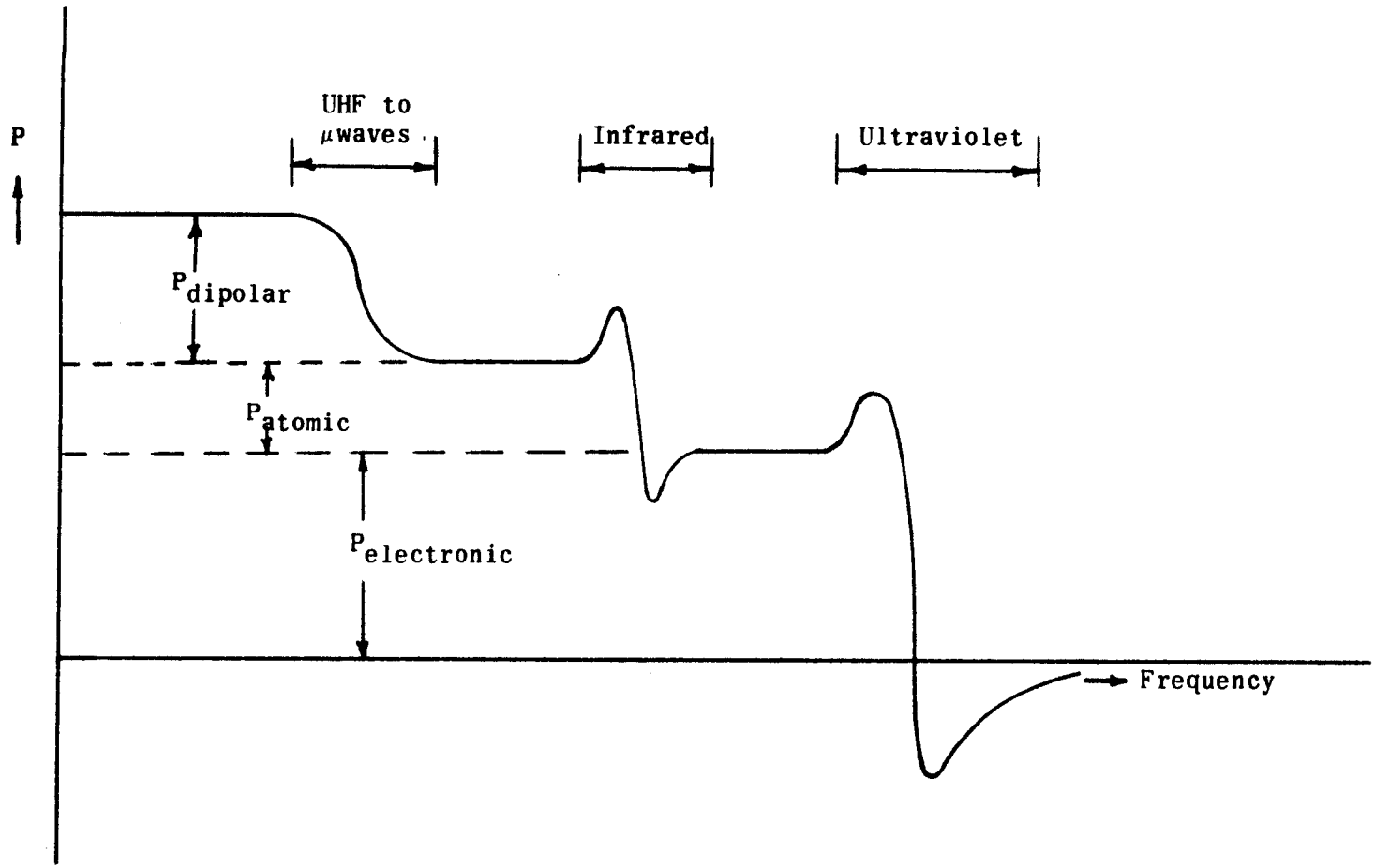

Figure 1.- The real part of the total polarization P as function of frequency for a dipolar substance with a single atomic and electronic resonance frequency.

of the medium by artificial dielectrics.[2] However, the dielectric constant and loss tangent of many materials in the microwave region are found experimentally using resonant cavity techniques.[3]

Langley Research Center (LRC) employs many dielectric materials for antenna windows, radome covers, and other applications. With the trend toward higher frequencies for space telemetry and communication, it is very important that the properties of such materials be known in the millimeter region.

In the millimeter and submillimeter wavelength regions conventional microwave cavity resonators become increasingly difficult to construct while maintaining reasonable tolerances and relative high Q's, because their dimensions must be comparable to the operating wavelength. Cylindrical waveguide cavities are normally used for the measurements of dielectric constants and losses at low microwave frequencies, but such devices are limited in the millimeter region because a relative high Q can not be maintained due to side wall losses and mechanical tolerances. Also, the samples used must have dimensions which are the same as the cavity itself. To avoid such intolerable dimensions, to increase the value of Q, and to increase the accuracy of the test data resonators must be constructed with dimensions many times larger than the operating wavelength.

---

[2]John D. Kraus, Electromagnetics (New York: McGraw-Hill Book Company, Inc., 1953), pp. 56-59.

[3]Carol G. Montgomery, Techniques of Microwave Measurements (New York: McGraw-Hill Book Company, Inc., 1947), pp. 657-665.

One method that has received considerable attention[4,5,6] which could act as a suitable resonator, especially in the millimeter and submillimeter region, is the Fabry-Perot interferometer, shown in Figure 2. The advantage of such an interferometer in the millimeter region is that its physical dimensions are large compared to the operating wavelength and the maintainance of high Q is made much easier.

The use of such a device for the measurements of dielectric constants and losses[7] in the millimeter region is ideal, because a sample of large dimensions can be used. The mathematical treatment of the dielectric constants and losses using the interforemeter is based upon the excitation of plane waves. To assure that plane waves are excited, collimating lens are used to convert the spherical waves to plane waves. Thin perforated membranes are used as reflectors, and the holes are used to couple energy in and out of the resonator.

---

[4] W. Culshaw, "Resonators for Millimeter and Submillimeter Wavelengths," IRE Transactions on Microwave Theory and Techniques, 9:135-144, March, 1961.

[5] _____, "High Resolution Millimeter Wave Fabry-Perot Interferometer," United States Department of Commerce, National Bureau of Standards, NBS Report 6039:1-32.

[6] R. W. Zimmerer; M. V. Anderson; G. L. Strine; and Y. Beers, "Millimeter Wavelength Resonant Structures," IEEE Transactions on Microwave Theory and Techniques, 11:142-149, March, 1963.

[7] W. Culshaw; and M. V. Anderson, "Measurements of Dielectric Constants and Losses with a Millimeter Wave Fabry-Perot Interferometer," United States Department of Commerce, Boulder, Colo., NBS Report 6786, July 19, 1961.

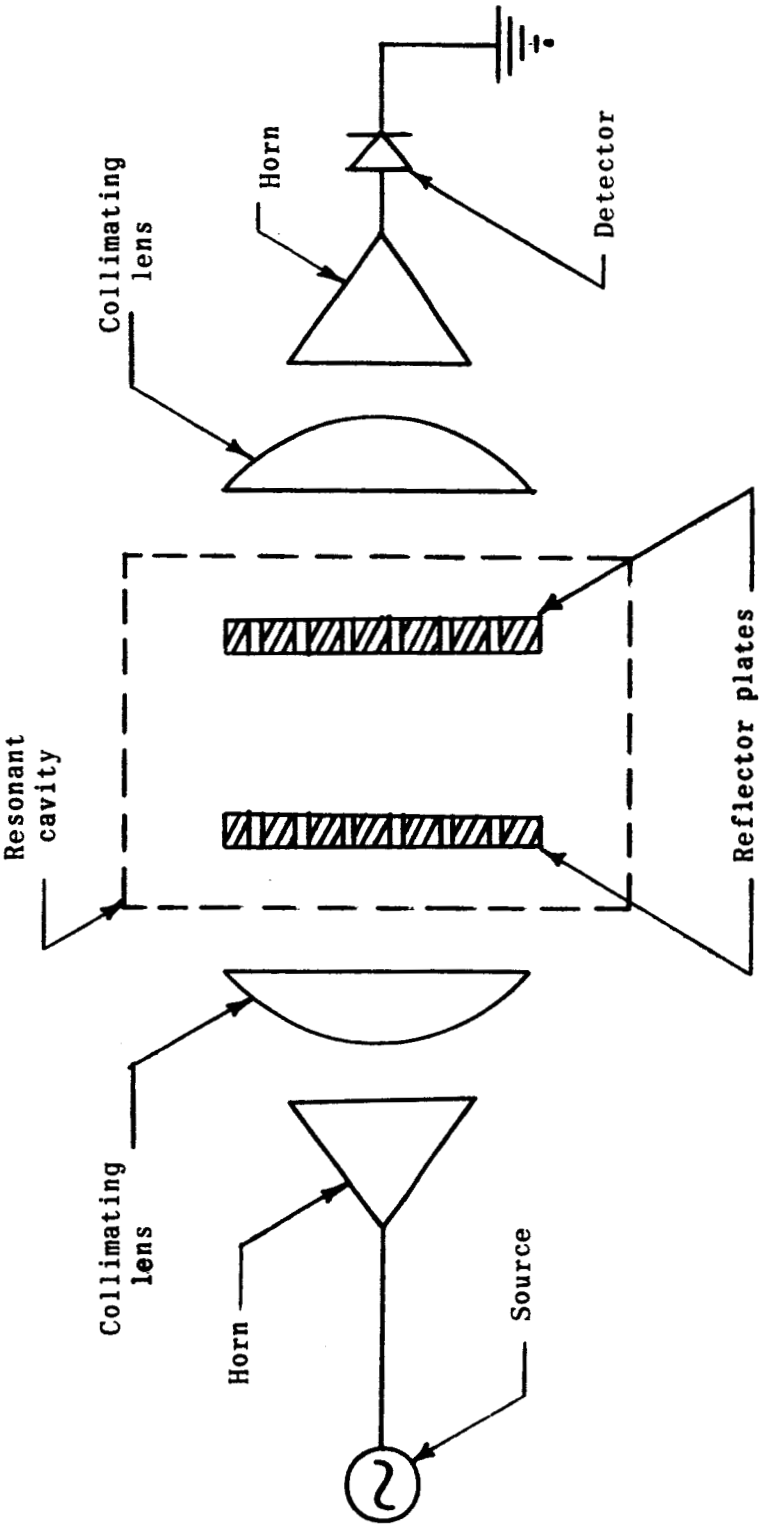

Figure 2.- Flat-plate Fabry-Perot interferometer.

To further verify the application of such a device, a modified system was used for the measurements of dielectric constants and loss tangents at higher millimeter frequencies. To verify the theory, samples of different thicknesses were used and the results compared. To determine data accuracy, samples of various surface finishes were employed. This was undertaken to determine the surface finish necessary to insure good data for practical applications.

CHAPTER II

INTERFEROMETER RESONANCE THEORY

The resonance of a Fabry-Perot resonant cavity is a function of plate separation.[8] Once a resonance is obtained, the insertion of a dielectric slab between the plates will disturb its resonance, but a shift in plate position will restore it. The equation defining interferometer resonance having a dielectric material between its plates can be derived using impedance transformations.

Impedance Transformation Method

The interferometer resonance equation is derived using transmission line theory assuming that a lossless medium ($\alpha = 0$) is present between the plates. The resonant cavity with the dielectric slab between its plates is shown in Figure 3(a). Assuming plane waves, the fields in the various regions can be expressed as

$$\left.\begin{aligned} E_o &= A_o\, e^{j(\omega t-\beta x)} + B_o\, e^{j(\omega t+\beta x)} \\ H_o &= 1/Z_o \left[A_o\, e^{j(\omega t-\beta x)} - B_o\, e^{j(\omega t+\beta x)} \right] \end{aligned}\right\} \begin{array}{l} \text{Region no. 1} \\ 0 \le x \le x_1 \end{array} \qquad (1)$$

$$\left.\begin{aligned} E_1 &= A_1\, e^{j(\omega t-\beta_1 x)} + B_1\, e^{j(\omega t+\beta_1 x)} \\ H_1 &= 1/Z_1 \left[A_1\, e^{j(\omega t-\beta_1 x)} - B_1\, e^{j(\omega t+\beta_1 x)} \right] \end{aligned}\right\} \begin{array}{l} \text{Region no. 2} \\ x_1 \le x \le x_2 \end{array} \qquad (2)$$

---

[8] See Appendix I.

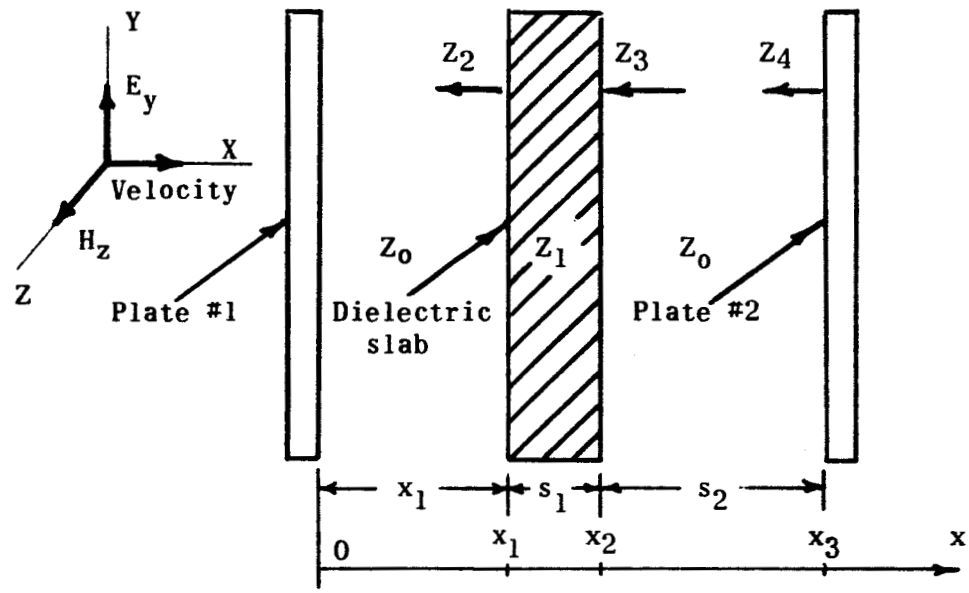

(a) Resonance with dielectric slab.

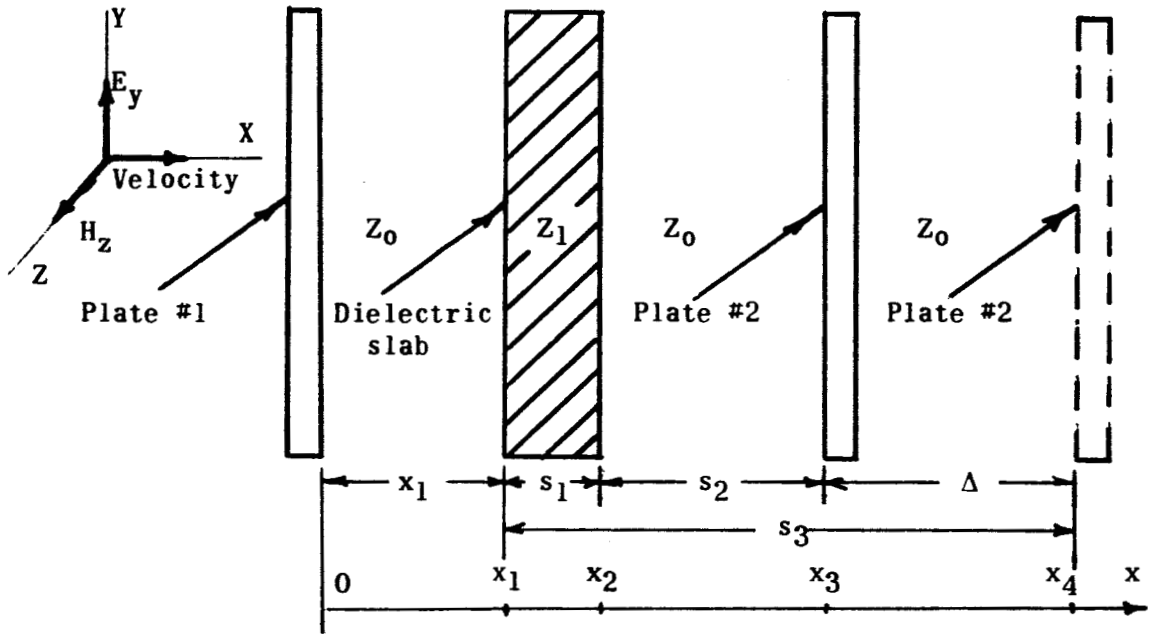

(b) Resonance with and without dielectric slab.

Figure 3.- Relative positions of reflector plates and slab for resonance.

$$\left.\begin{aligned} E_2 &= A_2\, e^{j(wt-\beta x)} + B_2\, e^{j(wt+\beta x)} \\ H_2 &= 1/Z_o\left[A_2\, e^{j(wt-\beta x)} - B_2\, e^{j(wt+\beta x)}\right] \end{aligned}\right\} \begin{array}{l}\text{Region no. 3} \\ x_2 \le x \le x_3\end{array} \tag{3}$$

where Z_o and Z_1 are the intrinsic impedances in their respective regions defined as

$$Z_o = \left(\mu_o/\epsilon_o\right)^{1/2} \tag{4}$$

$$Z_1 = \left(\mu_1/\epsilon_1\right)^{1/2} \tag{5}$$

The standing wave equations for each region can be written as

$$\left.\begin{aligned} E_o &= \left[\left(A_o + B_o\right)\cos\beta x - j\left(A_o - B_o\right)\sin\beta x\right] \\ H_o &= 1/Z_o\left[\left(A_o - B_o\right)\cos\beta x - j\left(A_o + B_o\right)\sin\beta x\right] \end{aligned}\right\} \begin{array}{l}\text{Region no. 1} \\ 0 \le x \le x_1\end{array} \tag{6}$$

$$\left.\begin{aligned} E_1 &= \left[\left(A_1 + B_1\right)\cos\beta_1 x - j\left(A_1 - B_1\right)\sin\beta_1 x\right] \\ H_1 &= 1/Z_1\left[\left(A_1 - B_1\right)\cos\beta_1 x - j\left(A_1 + B_1\right)\sin\beta_1 x\right] \end{aligned}\right\} \begin{array}{l}\text{Region no. 2} \\ x_1 \le x \le x_2\end{array} \tag{7}$$

$$\left.\begin{aligned} E_2 &= \left[\left(A_2 + B_2\right)\cos \beta x - j\left(A_2 - B_2\right)\sin \beta x\right] \\ H_2 &= 1/Z_o\left[\left(A_2 - B_2\right)\cos \beta x - j\left(A_2 + B_2\right)\sin \beta x\right] \end{aligned}\right\} \begin{array}{l}\text{Region no. 3} \\ x_2 \le x \le x_3\end{array} \quad (8)$$

For resonance, an electric field node or a magnetic field antinode must exist at $x = 0$ and $x = x_4 = n\pi$. Therefore, $B_o = -A_o$ and $B_2 = -A_2$. Equations (6), (7), and (8) can then be expressed as

$$\left.\begin{aligned} E_o &= -j2A_o \sin \beta x \\ H_o &= 1/Z_o\left[2A_o \cos \beta x\right] \end{aligned}\right\} \begin{array}{l}\text{Region no. 1} \\ 0 \le x \le x_1\end{array} \quad (9)$$

$$\left.\begin{aligned} E_1 &= -j2A_1 \sin \beta_1 x \\ H_1 &= 1/Z_1\left[2A_1 \cos \beta_1 x\right] \end{aligned}\right\} \begin{array}{l}\text{Region no. 2} \\ x_1 \le x \le x_2\end{array} \quad (10)$$

$$\left.\begin{aligned} E_2 &= -j2A_2 \sin \beta x \\ H_2 &= 1/Z_o\left[2A_2 \cos \beta x\right] \end{aligned}\right\} \begin{array}{l}\text{Region no. 3} \\ x_2 \le x \le x_3\end{array} \quad (11)$$

These equations represent the fields in their respective regions during resonance.

The impedance seen at point x_1, looking towards reflector No. 1, is given by

$$Z_2 = Z_o \left[\frac{Z_L + jZ_o \tan \beta x_1}{Z_o + jZ_L \tan \beta x_1} \right] \tag{12}$$

Assuming an ideal short at reflector no. 1, equation (12) is expressed as

$$Z_2 = jZ_o \tan \beta x_1 \tag{13}$$

Such an assumption is valid because plates with reflection coefficients of 0.995 and better can be constructed. At $x = x_2$, the impedance Z_3 is given by

$$Z_3 = Z_1 \left[\frac{Z_2 + jZ_1 \tan \beta_1 s_1}{Z_1 + jZ_2 \tan \beta_1 s_1} \right] \tag{14}$$

and at $x = x_3$, Z_4 is expressed by

$$Z_4 = Z_o \left[\frac{Z_3 + jZ_o \tan \beta s_2}{Z_o + jZ_3 \tan \beta s_2} \right] \tag{15}$$

For interferometer resonance, an electric field node must exist at $x = x_4$; i.e., Z_4 must be equal to zero. Equation (15) can then be expressed as

$$Z_3 + jZ_o \tan \beta s_2 = 0 \tag{16}$$

Substituting Equation (13) into equation (14) gives

$$Z_3 = jZ_1 \left[\frac{Z_o \tan \beta x_1 + Z_1 \tan \beta_1 s_1}{Z_1 - Z_o \tan \beta x_1 \tan \beta_1 s_1} \right] \tag{17}$$

Equation (17) can now be inserted into equation (16), and the equation defining resonance is given by

$$\left(\frac{Z_0}{Z_1}\right) \cot \beta_1 s_1 \left[\cot \beta s_2 + \cot \beta x_1\right] + \cot \beta x_1 \cot \beta s_2 - \left(\frac{Z_0}{Z_1}\right)^2 = 0 \tag{18}$$

Defining $Z_o/Z_1 = k$, equation (18) can be expressed as

$$k \cot \beta_1 s_1 \left[\cot \beta s_2 + \cot \beta x_1\right] + \cot \beta x_1 \cot \beta s_2 - k^2 = 0 \tag{19}$$

By direct measurement of the relative distances between the slab and the plates, and slab thickness, the value of k can be found using equation (19). The expression defining k is given by

$$k = \left(Z_o/Z_1\right) = \left[\frac{\mu_o/\epsilon_o}{\mu_1/\epsilon_1}\right]^{1/2} = \left[\frac{\mu_o \epsilon_1}{\mu_1 \epsilon_o}\right]^{1/2} \tag{20}$$

Since for most nonferrous materials $\mu_o \approx \mu_1$,[9] equation (20) can be expressed as

$$k = \left(\epsilon_1/\epsilon_o\right)^{1/2} = (\epsilon)^{1/2} \tag{21}$$

---

[9] Derived equations will not apply for highly conducting slabs.

Knowing k, the dielectric constant ϵ, can be found. It should be noted that equation (19) is a transcendental equation and many values of k will satisfy it. Equation (19) can be derived in another way by using equations (9), (10), and (11) and applying boundary conditions at points of discontinuity.[10,11]

Dielectric Constant Determination

Once a resonance has been achieved, the insertion of a dielectric will alter the resonant length of the cavity and a shift in position of one of the reflectors must be made in order to restore resonance. Referring to Figure 3(b), the dashed plate represents the position of plate no. 2 for resonance before the insertion of the dielectric, and the solid its position for resonance after the insertion of the dielectric.

Before the insertion of the dielectric $x = 0$ and $x = x_4$ are electric field nodes; therefore

$$x_1 + s_3 = x_4 = n\pi/\beta \qquad n = 1, 2, 3, \cdots \qquad (22)$$

Substitution of equation (22) into equation (19) results in

$$k \cot \beta_1 s_1 \left[\cot \beta s_3 - \cot \beta s_2\right] + \cot \beta s_3 \cot \beta s_2 + k^2 = 0 \qquad (23)$$

---

[10] H. R. L. Lamont, "Theory of Resonance in Microwave Transmission Lines with Discontinuous Dielectric," Philosophical Magazine, Series 7, vol. 29, No. 197:521-531, June, 1940.

[11] W. Culshaw and M. V. Anderson, op.cit. pp. 5-9.

If Λ is the shift of plate no. 2 to restore resonance then

$$s_2 = s_3 - (s_1 + \Delta) \tag{24}$$

Substitution of equation (24) into equation (23) yields

$$k \cot \beta_1 s_1 \left\{ \cot \beta s_3 - \cot \left[s_3 - (s_1 + \Lambda) \right] \right\} + \cot \beta s_3 \cot \beta \left[s_3 - (s_1 + \Delta) \right] + k^2 = 0 \tag{25}$$

Using equation (25) a curve of Δ versus s_3 can be drawn. It has been shown[12] that the turning points of this curve are given by

$$\tan \beta s_3 = 1/k \left[\tan \left(\tfrac{1}{2} \beta_1 s_1 \right) \right] \tag{26}$$

and

$$\tan \beta s_3 = - 1/k \left[\cot \left(\tfrac{1}{2} \beta_1 s_1 \right) \right] \tag{27}$$

and the corresponding values of Δ by

$$\tan \tfrac{1}{2} \beta (s_1 + \Delta) = 1/k \left[\tan \left(\tfrac{1}{2} \beta_1 s_1 \right) \right] \tag{28}$$

$$\tan \tfrac{1}{2} \beta (s_1 + \Delta) = k \left[\tan \left(\tfrac{1}{2} \beta_1 s_1 \right) \right] \tag{29}$$

Which of equations (28) and (29) represents Δ_{max} and which Δ_{min} depends on the sign of $\tan \frac{\beta_1 s_1}{2}$, i.e., upon the thickness s_1 of the slab. Since $k > 1$, it is evident that when the integral part of

---

[12] H. R. L. Lamont, op. cit. p. 525.

$\left[\frac{2s_1}{\lambda_1}\right]$ is zero or even integer equation (28) gives Δ_{min} and equation (29) $\wedge_{max}$; when the integral part of $\left[\frac{2s_1}{\lambda_1}\right]$ is an odd integer equation (28) gives Δ_{max} and equation (29) Δ_{min}.

Another form of equation (25) is given by

$$\tan \beta\left(s_1 + \Delta\right) = \tan \beta_1 s_1 \left[\frac{\cot \beta s_3 + k^2 \tan \beta s_3}{k\left(\tan \beta s_3 + \cot \beta s_3\right) + \left(k^2 - 1\right) \tan \beta_1 s_1}\right] \quad (30)$$

When the thickness of the dielectric slab is an integral number of half-wavelengths, or

$$\beta_1 s_1 = n\pi = n\lambda/2 \qquad n = 1, 2, 3, \cdots \quad (31)$$

then equation (29) is equal to

$$\tan \beta \left(s_1 + \wedge\right) = \tan \beta_1 s_1 = 0$$

$$\beta\left(s_1 + \Delta\right) = \beta_1 s_1 = n\pi$$

$$\Delta = s_1 (k - 1) \quad (32)$$

Examining equation (19), which describes the interferometer resonance when the dielectric slab is between the plates, it can be concluded that there is a linear relation between x_1 and s_2 when the dielectric thickness is a multiple of a half-wavelength. Such a relation is given by

$$\cot \beta s_2 = - \cot \beta x_1$$

$$\beta s_2 = - \beta x_1 + n\pi \quad n = 0, \pm 1, \pm 2, \ldots$$

$$x_1 + s_2 = n\lambda/2 \quad n = 0, \pm 1, \pm 2, \ldots \quad (33)$$

Thus, when $\beta_1 s_1 = n\pi$, the condition for resonance depends upon the sum of the distances s_2 and x_1, as given by equation (33). Once resonance has been restored after the insertion of the slab, a change in the position of the slab will not disturb resonance, as long as equations (31) and (33) are satisfied. This can better be understood by remembering, from impedance transformation techniques, that layers of multiples of half-wavelengths thick produce no change in the impedance seen before and after them. The Δ required to restore resonance will be the same for any position of the dielectric, assuming that equation (31) is satisfied.

Therefore, there is evidence that there are at least three possible methods of determining the dielectric constant of a slab.[13] The first and most direct method would be to use equation (19). By directly measuring distances x_1, s_2, and s_1, and knowing the operating wavelength, the value of k can be found. A computer program would more accurately determine k.

---

[13] W. Culshaw and M. V. Anderson, op. cit. pp. 11-12.

A second method is to plot Δ versus s_3 for each dielectric slab. The values of Δ will oscillate between Δ_{max} and Δ_{min} as a function of s_3. Once Δ_{max} and Δ_{min} have been determined, k can be found using equations (28) and (29). A computer program is also recommended in accurately determining k using this method.

The third method would be to use slabs whose thicknesses are multiples of half-wavelengths. By measuring Δ, the shift of position of plate no. 2 to restore resonance, k can be determined using equation (32). This probably would be the easiest method for determining k as long as slabs of multiples of half-wavelengths are available or when the primary source oscillates at frequencies which make the slabs multiples of half-wavelengths. At lower microwave frequencies such a problem is not very difficult. However, at the millimeter region the problem is somewhat more difficult.

Loss Tangent Evaluation

Most resonators are usually judged by their quality factor, or Q, which is defined as

$$Q = w \frac{\text{Energy stored}}{\text{Mean dissipation of power}} \tag{34}$$

The average power loss or the dissipated power in the cavity is given by

$$P_s = \frac{R_s}{2} \iint_{\text{cavity walls}} H_{tan} \cdot H^*_{tan} \, dS \tag{35}$$

where R_s is the real part of the surface impedance of the plates, and H_{tan} is the magnetic field tangential to the plate surfaces. The maximum stored energy W in a cavity resonator of any arbitrary shape for a sinusoidally time-varying field is given by

$$W_s = \frac{\epsilon}{2}\iiint_V E \cdot E^* \, dV = \frac{\mu}{2}\iiint_V H \cdot H^* \, dV \tag{36}$$

where V denotes the volume of the cavity. Thus, if the field distribution inside the cavity is known, the Q can be evaluated regardless of its shape or size. Also knowing the field distribution, the resonant frequency can be determined. The field distribtuion for many shapes of cavities are difficult to determine. However, for some simple geometrical shapes of a cavity, it is possible to estimate the field distribution, and hence determine the Q and the resonant frequency fairly accurately. The dimensions of the inner and outer conductors must be assumed to be such that higher order modes, other than the TEM mode, do not exist inside the cavity. The equations derived previously in each region can now be used to derive the Q of the cavity with and without the dielectric. Assuming that there is a lossless medium between the plates, the energy stored is given by

$$W_s = \frac{\epsilon_o}{2}\iiint_V E_o \cdot E_o^* \, dV$$

$$W_s = \frac{\epsilon_o}{2} \iiint_V 4 A_o^2 \sin^2 \beta x \, dV \tag{37}$$

Remembering that for resonance $d = n\pi$, equation (37) can be written as

$$W_s = \epsilon_o d A_o^2 \iint_A dS \tag{38}$$

The average power loss or the dissipated power in the cavity per plate is given by

$$P_s = \frac{R_s}{2} \iint_A H_{tan} \cdot H^*_{tan} \, dS$$

$$P_s = \frac{2A_o^2 R_s}{Z_o^2} \iint_A \cos^2 \beta x \, dS \tag{39}$$

Since the surfaces of the reflector plates at resonance are at distances equal to $x = o$ and $x = n\pi$, equation (39) can be written as

$$P_s = \frac{2A_o^2 R_s}{Z_o^2} \iint_A dS \tag{40}$$

The above equation represents losses per plate. Assuming that the losses in both plates are equal, the equation representing the total dissipated power by the plates is given by

$$P_s = \frac{4A_o^2 R_s}{Z_o^2} \int_A \int dS \tag{41}$$

The Q of the cavity without any dielectric between the plates is obtained by using the basic definition given by equation (34) and substituting equations (38) and (41), as represented by

$$Q_o = \frac{w\epsilon_o d}{4R_s/Z_o^2} \tag{42}$$

Equation (42) represents the Q_o of the cavity when there are no diffraction losses from the sides of the interferometer. The evaluation of the Q is simplified[14] by assuming that the diffraction losses with and without the dielectric are the same, and that slabs whose thicknesses are multiples of half-wavelengths are used.

To account for diffraction losses, an additional term P_d is added in equation (42), thus expressing the Q of the cavity without the dielectric as

$$Q_o = \frac{w\epsilon_o d}{4R_s/Z_o^2 + P_d} \tag{43}$$

The radiation resistance of the cavity due to transmission through the end plates is also included in P_d. Once the dielectric is inserted between the plates the Q of the cavity will be reduced and is given by

---

[14] Ibid., pp. 13-15.

$$Q_t = \frac{w\left\{\frac{\epsilon_o}{2}\int_A dS \int_o^{x_1} |E_o|^2\, dx + \frac{\epsilon'}{2}\int_A dS \int_{x_1}^{x_2} |E_1|^2\, dx + \frac{\epsilon_o}{2}\int_A ds \int_{x_2}^{x_3} |E_2|^2 dx\right\}}{\frac{w\epsilon''}{2}\int_A dS \int_{x_1}^{x_2} |E_1|^2\, dx + \frac{R_s}{2}\int_A |H_o|^2\, dS + \frac{R_s}{2}\int_A |H_2|^2\, dS + P_d A_o \int_A dS} \tag{44}$$

The evaluation of equation (44) using the expression for the fields derived previously is quite complicated. If sheets whose thicknesses are multiples of half-wavelengths are available, the evaluation becomes simplified and is given by

$$Q_t = \frac{w\left\{\epsilon_o A_o^2 (x_1 + s_2) + \epsilon' s_1 A_o^2 \left(k^{-2}\cos^2 \beta_1 x_1 + \sin^2 \beta_1 x_1\right)\right\}}{we'' s_1 A_o^2 \left(k^{-2}\cos^2 \beta_1 x_1 + \sin^2 \beta_1 x_1\right) + 4A_o^2 R_s / Z_o^2 + P_d A_o^2} \tag{45}$$

where $\epsilon = \epsilon' + j\epsilon''$ is the complex dielectric constant and $\tan \delta = \frac{\epsilon''}{\epsilon'}$. Assuming that dielectric losses exceed resistive and diffraction losses, the maximum value of equation (45) occurs when $\beta x_1 = n\pi$ and is given by

$$\frac{1}{Q_{tmax}} = \frac{1}{Q_o} + \tan \delta \left(\frac{s_1}{d} \right) \tag{46}$$

where $d = x_1 + s_1 + s_2$.

CHAPTER III

SYSTEM DESCRIPTION

The photograph of the system used for the measurements of the dielectric constant and loss tangent is shown in Figure 4. A block diagram of this system is shown in Figure 5.

The basic frame of the interferometer is about 36 inches long. Two upright frames are used to support the reflector plates. Each frame has various tilt adjustments, and it can be moved forwards or backwards. The middle upright frame is used to support the dielectric slabs. It also has various tilt adjustments and can be moved in any direction. The aperture of the middle frame is 10 x 10 inches, and dielectric slabs much larger than the size of the reflector plates can be used. This is to insure that the basic structure would not interfere with the propagation of the waves.

The horn antennas have an aperture of 2-1/8 x 2-1/8 inches. The dielectric lenses were used to convert spherical waves to plane waves. The profile of lenses necessary for such conversion should be hyperbolic. However, because of the difficulty in constructing such a profile, a spherical approximation was used. The equation defining such an approximation is given by

$$\frac{1}{L} = \frac{k - 1}{R} \tag{47}$$

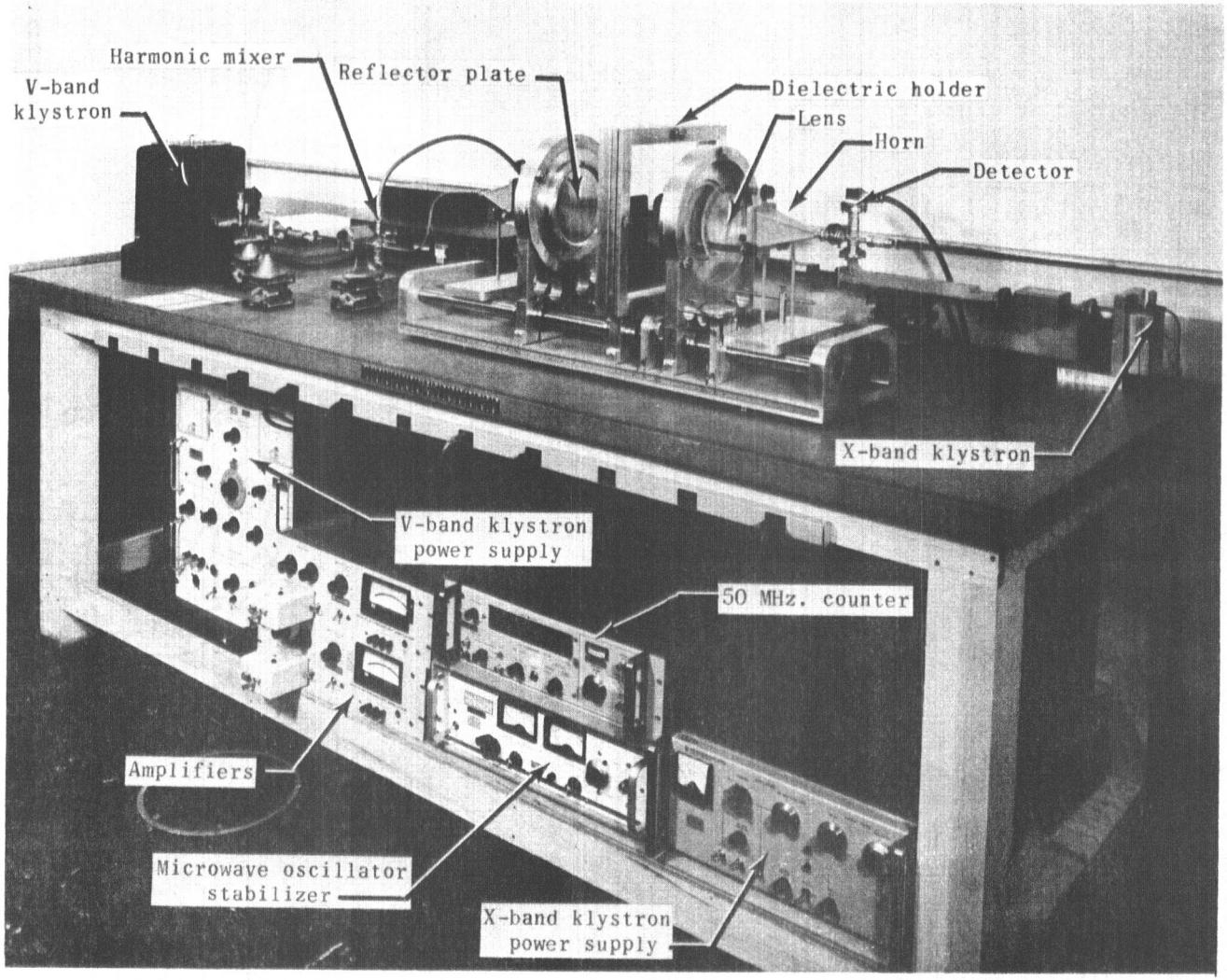

Figure 4.- System used for the measurements of dielectric constant and loss tangent at millimeter region.

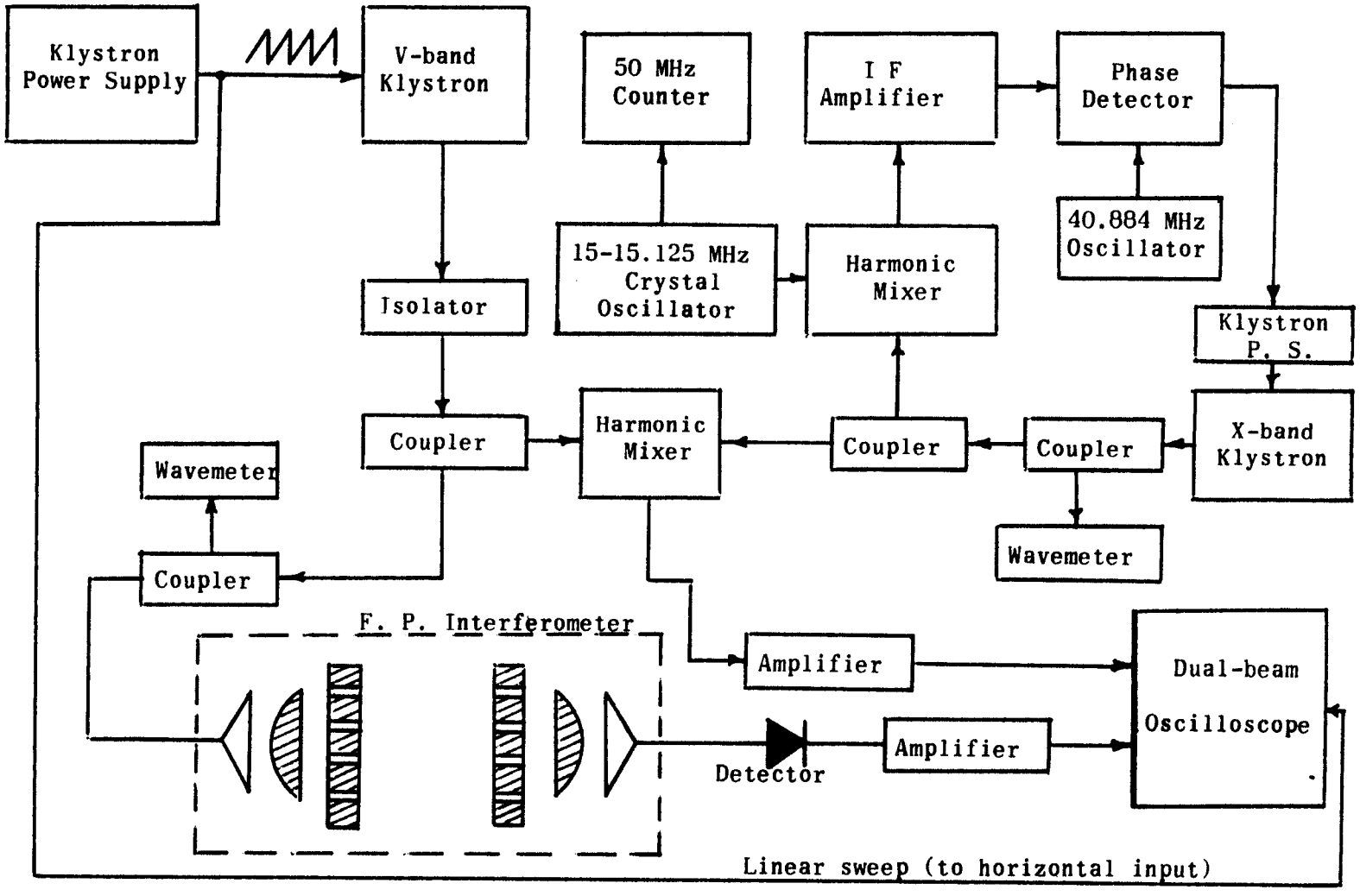

Figure 5.- Block diagram of system for measurement of dielectric constant and loss tangent at millimeter region.

Where: L - focal length
R - radius of curvature of lens
k - index of refraction of the dielectric lens

The lenses were made out of rexolite which has an index of refraction of about 1.57. A focal length of 5.9 inches was assumed, thus giving a radius of curvature of about 3.36 inches.

For reflector plates, thin perforated membranes[15] were used. The thickness of the membranes was about 0.001 inches. The membranes were made of nickel coated with a thin film of gold to increase the conductivity of the surface. A photoetching process was adopted[16] for the construction of the membranes. The membranes are circular in shape with a diameter of about five inches.

A photograph of the membrane with its hole pattern used in the tests is shown in Figure 6. The hole pattern of the perforated membranes is better shown in Figure 7. Since it was necessary not only to obtain a relative high Q but also good transmission, a compromise in the design of the reflector plates was made. The relative dimensions of the perforated plates are given by a = b = 0.1 inches and r = 0.02 inches. A transmission loss of 23.36 dB per plate was calculated.[17]

---

[15] R. W. Zimmerer; M. V. Anderson; G. L. Strine; and Y. Beers, op. cit. p. 142.

[16] Custom Microwaves, Longwood, Florida.

[17] R. W. Zimmerer; M. V. Anderson; G. L. Strine; and Y. Beers, op. cit. pp. 143-144.

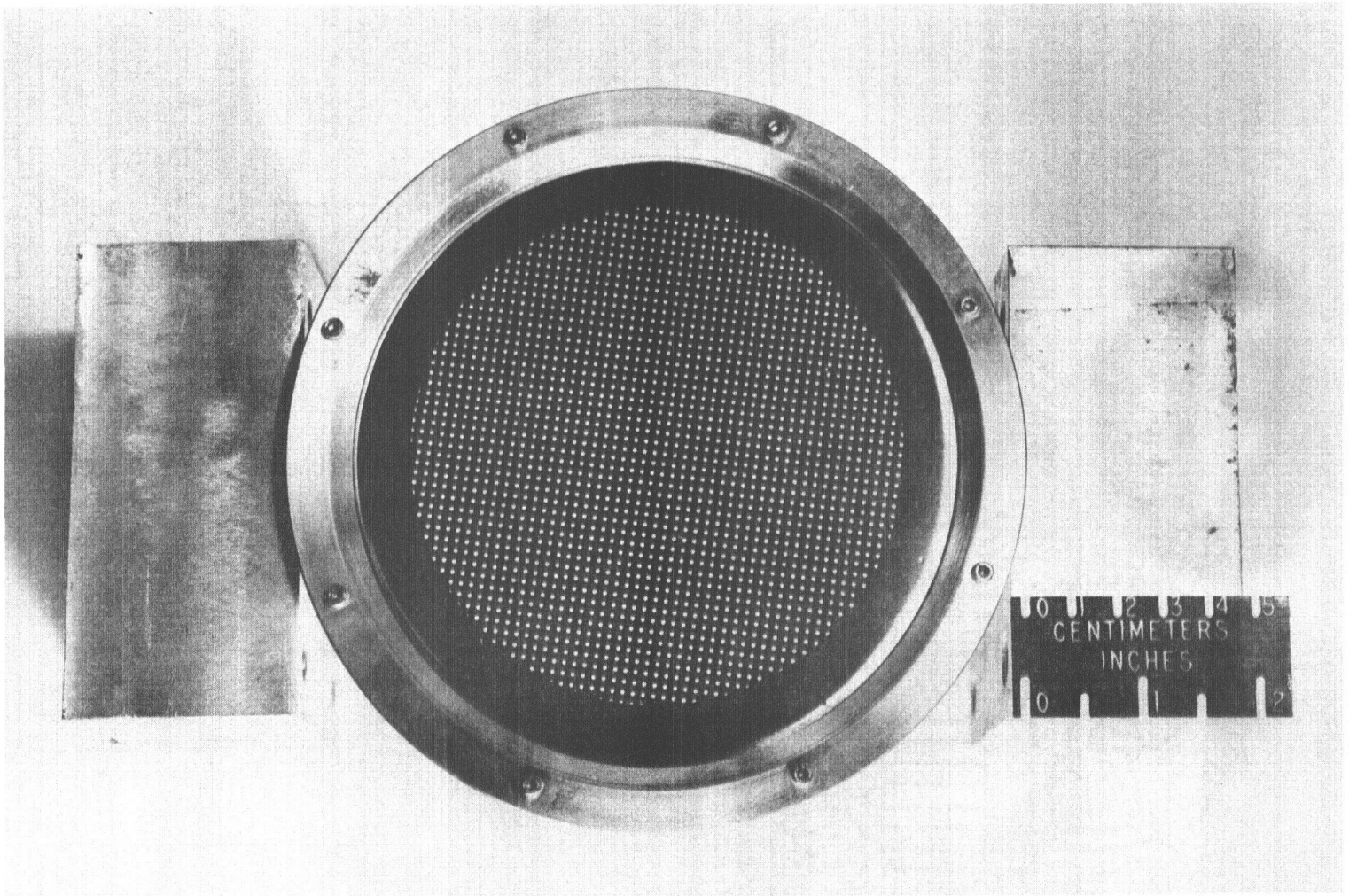

Figure 6.- Perforated reflector plate.

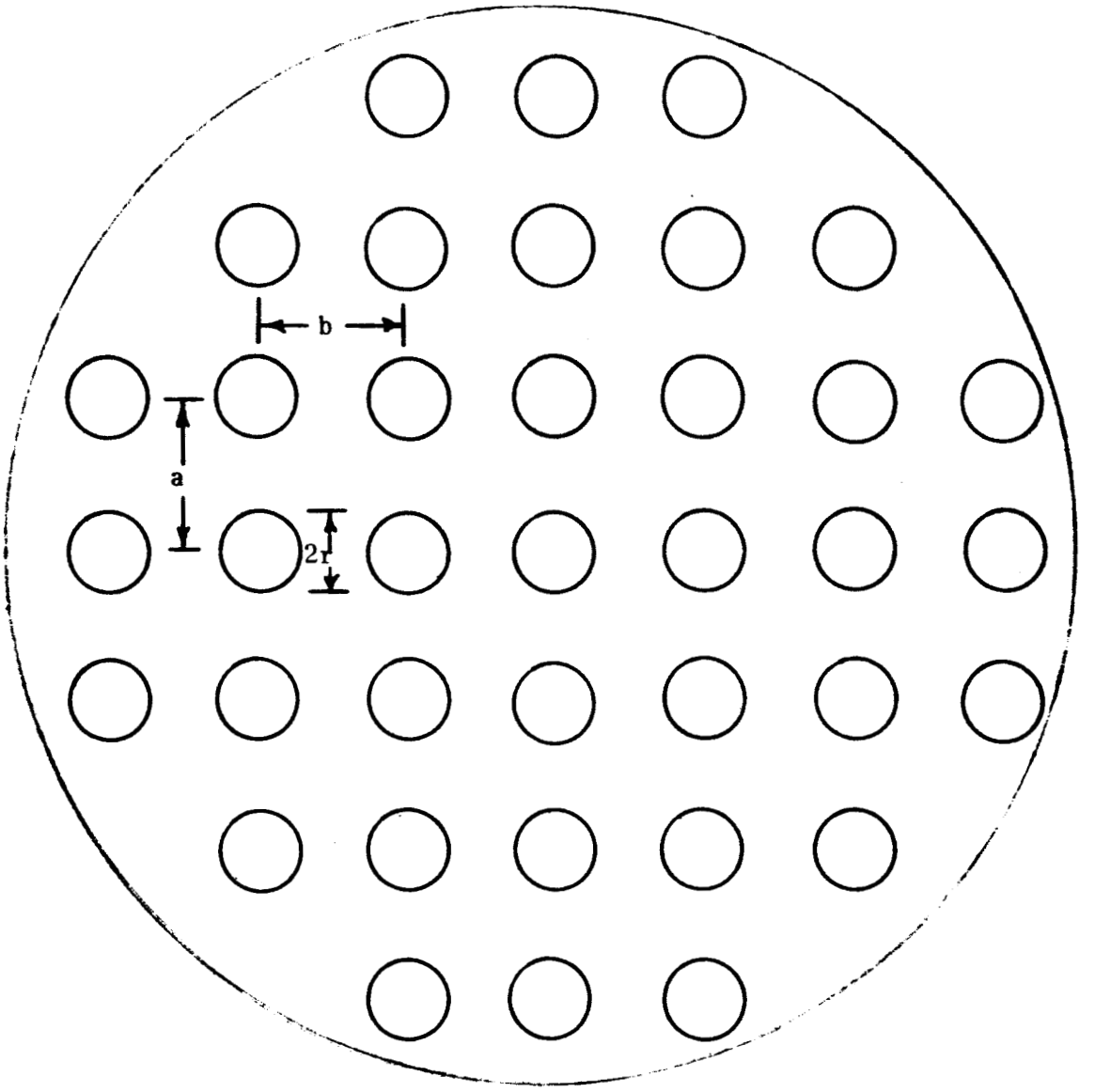

Figure 7.- Hole pattern of reflector plate.

The measured loss per plate was about 18.5 dB and of the entire system about 8.5 dB. The design was centered around 60 GHz.

Conventional methods employed for the measurements of Q at lower microwave frequencies can not be used in the millimeter region since accurate wavemeters are not presently available. A system using a different technique has been used to measure the Q and is shown in Figure 5. The 60 GHz klystron is linearly varied through a frequency range, and the response of the Fabry-Perot resonant cavity is displayed on the oscilloscope. Such a response curve is shown in Figure 8(a). A portion of the output of the 60 GHz klystron is mixed with the sixth harmonic of a phase-locked X-band source. The X-band source is varied until a zero beat is detected from the harmonic mixer. The zero beat is displayed simultaneously on a dual beam oscilloscope with the response of the cavity, and it is used as a variable marker which is tuned to the center frequency and then to each of the half-power bandwidth points of the response curve. The zero beat used as a frequency marker is shown in Figure 8(b). The marker is determined for each case by measuring the frequency of the 15-15.125 MHz R F reference crystal oscillator with a 50 MHz counter thus permitting accurate determination of the center frequency and the half-power bandwidth points of the cavity response. The Q of the cavity is then determined by

$$Q = \frac{f_o}{\Delta f} \tag{48}$$

Where: f_o - center frequency of the cavity response
ΔF - half-power bandwidth of cavity response

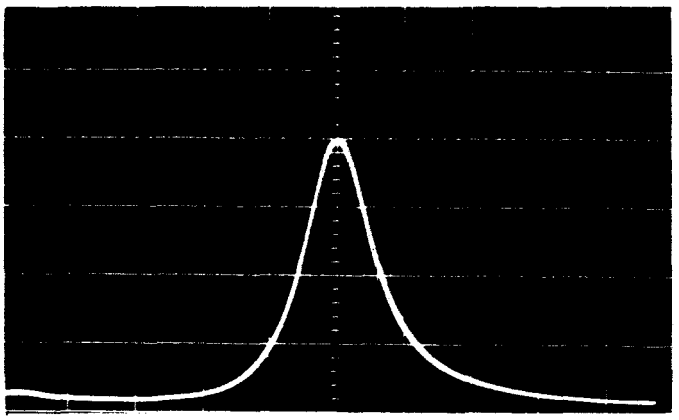

(a) Cavity response curve with air. Q = 10,960.

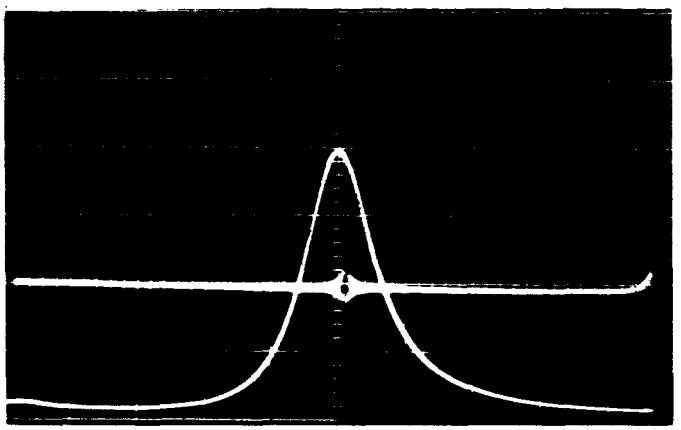

(b) Cavity response curve and zero beat used as a variable frequency marker. Q = 10,960.

Figure 8.- Cavity response curve and variable frequency marker.

CHAPTER IV

SYSTEM PERFORMANCE AND EXPERIMENTAL RESULTS

The purpose of this chapter is to discuss the tests performed, the methods used for the calculation of the dielectric constant and loss tangent, the experimental procedure for each method, problems encountered and the solutions employed. Included will be diagrams of experimental data, comparison of results with data at lower frequencies, and comparison of experimental diagrams with theoretically predicted curves. The theoretical prediction of the dielectric constants and loss tangents as function of frequency and temperature is very difficult if not impossible. However, factors which directly contribute to these parameters have been predicted theoretically and diagrams are available. It is the purpose to try to compare the results and previous existing data at lower frequencies with the theoretical predictions and comment on the shape of the experimental diagrams.

Dielectric Constant Measurements

Two methods were used for determining the dielectric constants. The first method was to use equation (32) assuming that equation (31) is satisfied, and the second to use equations (28) and (29). Since there are many values of k which will satisfy equations (28) and (29), it is recommended that the range of k be first determined by the use of equation (32); i.e., the first method should be used to determine the range of k for the different materials, and then the second

method can be used to verify the results. The experimental procedure and results for each method will be discussed.

First Method. To use this method for the measurement of dielectric constants, slabs whose thicknesses are multiples of half-wavelengths must be available. As will be shown later, the measurement of the loss tangent is based on the assumption that the slab thickness is a multiple of a half-wavelength; therefore, it will be advantageous to utilize such slabs, because they can be used for the measurements of the dielectric constant and loss tangent.

The experimental procedure for this method is as follows: First cause the cavity to resonate at the desired frequency. Display the response curve of the cavity on the oscilloscope. As the dielectric slab is inserted between the plates, the resonance will be disturbed, and the response curve will move or completely disappear from the oscilloscope. Move plate no. 2 toward plate no. 1 until resonance is restored (appearance of the response curve on the oscilloscope at the same position as previously). Record the Δ necessary to restore resonance, and by using equation (32) determine k. To make sure that the effective slab thickness is a multiple of a half-wavelength, move the dielectric slab in any direction and observe the response curve on the oscilloscope. There should be no movement of the response curve as the slab changes position. This can better be understood by remembering that the impedance seen looking toward plate no. 1 before and after

the slab is the same. Therefore, the position of the slab will have no effect as to the Δ required to restore resonance using this method.

As the slab thickness varies, Δ will also vary. If the slab thickness is more than one wavelength, the Δ which is used with equation (32) to determine k must carefully be selected.

When the response curve reappears on the oscilloscope after a shift of plate no. 2, the movement of plate no. 2 in the same direction will make the response curve reappear at succeeding intervals spaced one-half wavelength apart. Therefore, there are many Δ's which will restore resonance, and after the first they are spaced half-wavelengths apart.

It then becomes uncertain as to which Δ can safely be used with equation (32). This can be very confusing and could lead to erroneous results. To avoid possible errors, slabs of several thicknesses should be used and for each slab determine successive Δ's and their corresponding k's. By comparing the k's of different thickness slabs of the same material, it will be seen that there is only one value of k which is the same for each thickness. If however the slab thickness is equal to or less than one wavelength, the first Δ will be the one which gives the correct results.

The results obtained using this method are tabulated in Table I. The surface finish is represented by the symbol used by N A S A and S A E. It represents the average root-mean square height of surface irregularities in microinches.

TABLE I

DIELECTRIC CONSTANTS FOR VARIOUS MATERIALS OF SEVERAL THICKNESSES AND VARIOUS SURFACE FINISHES AT CONSTANT TEMPERATURE USING 1st METHOD

T E F L O N - 25 °C

Thickness / Surface Finish	1.0221±.005 ▽32	1.0922±.001 ▽16	1.6370±.001 ▽16	2.0877±.005 ▽32
Dielectric Constant	2.049	2.057	2.061	-----
Frequency MHz.	60,539.235	60,319.345	60,449.572	-----

P O L Y S T Y R E N E - 25 °C

Thickness / Surface Finish	0.9852±.001 ▽32	1.0123±.002 ▽64	1.4734±.001 ▽32	2,0100±.002 ▽130
Dielectric Constant	2.534	2.530	2.535	-------
Frequency MHz.	60,246.897	58,677.897	60,418.072	--------

P L E X I G L A S - 25 °C

Thickness / Surface Finish	0.1235±.002 ▽8	0.1831±.002 ▽8	0.3718±.003 ▽8
Dielectric Constant	2.578	2.594	------
Frequency MHz.	59,562.875	60,065.323	------

Second Method. Before this method can be used conveniently, it will be necessary that the range of the values of k be known. This can be done by the use of the first method. It must be pointed out that this is not necessary but convenient. As in the first method, there are many values which will satisfy equations (28) and (29), but there is only one value which will be the same for the different thickness slabs. However, the range of k can be determined much faster and more conveniently using the first method.

To use equations (28) and (29) for determining the dielectric constant, a plot of the shift of plate no. 2 necessary to restore resonance (Δ) versus dielectric position (s_3) must be drawn. This is done as follows: Display on the oscilloscope the response of the resonant cavity before the insertion of the dielectric. Upon the insertion of the dielectric, the resonance of the cavity is disturbed, and the response curve will move or completely disappear from the oscilloscope. Move plate no. 2 toward the dielectric slab until the response curve of the cavity reappears in its original position. As you begin to move the position of the slab in one direction, the response curve on the oscilloscope will also move. In order to keep the response curve always in the same position on the oscilloscope as the dielectric position is varied, the position of plate no. 2 must also be changed. Start moving the slab in one direction and observe the direction of movement of the response curve, left or right.

Simultaneously, move plate no. 2 in a direction such that the response curve will maintain its position. For each position of the dielectric slab record the position of plate no. 2. A plot of s_3 versus Δ for polystyrene is shown in Figure 9.

Once Δ_{max} and Δ_{min} were determined, an iterative procedure ideally suited for use with a computer was applied for determining k using equations (28) and (29)[18]. It must be remembered that whether you use equation (28) or equation (29) for Δ_{max} or Δ_{min} depends upon the integral part of $2s_1/\lambda_1$ as was stated previously. To avoid any possible errors, equations (28), (29) and $2s_1/\lambda_1$ were evaluated for each value of Δ_{max} and Δ_{min}. The correct value of k was then determined by checking each value of Δ_{max} or Δ_{min} against its corresponding value of $2s_1/\lambda_1$ to see that the integral part satisfies the conclusions drawn previously.

The values of Δ_{max} and Δ_{min} will not differ very much if the thickness of the slab is close to being an integral number of half-wavelengths. Again, when the slab thickness is equal to $n\lambda_1/2$, then $\Delta_{max} = \Delta_{min}$, or the shift necessary to restore resonance will be the same regardless of the position of the slab. Also, when the slab thickness is close to being equal to $n\lambda_1/2$, the ratio $2s_1/\lambda_1$ will very closely be equal to an integer. Using this method, the operating frequency should always be selected such that the effective thickness of the slab is not close to being an integral number of

---

[18] See Appendix II.

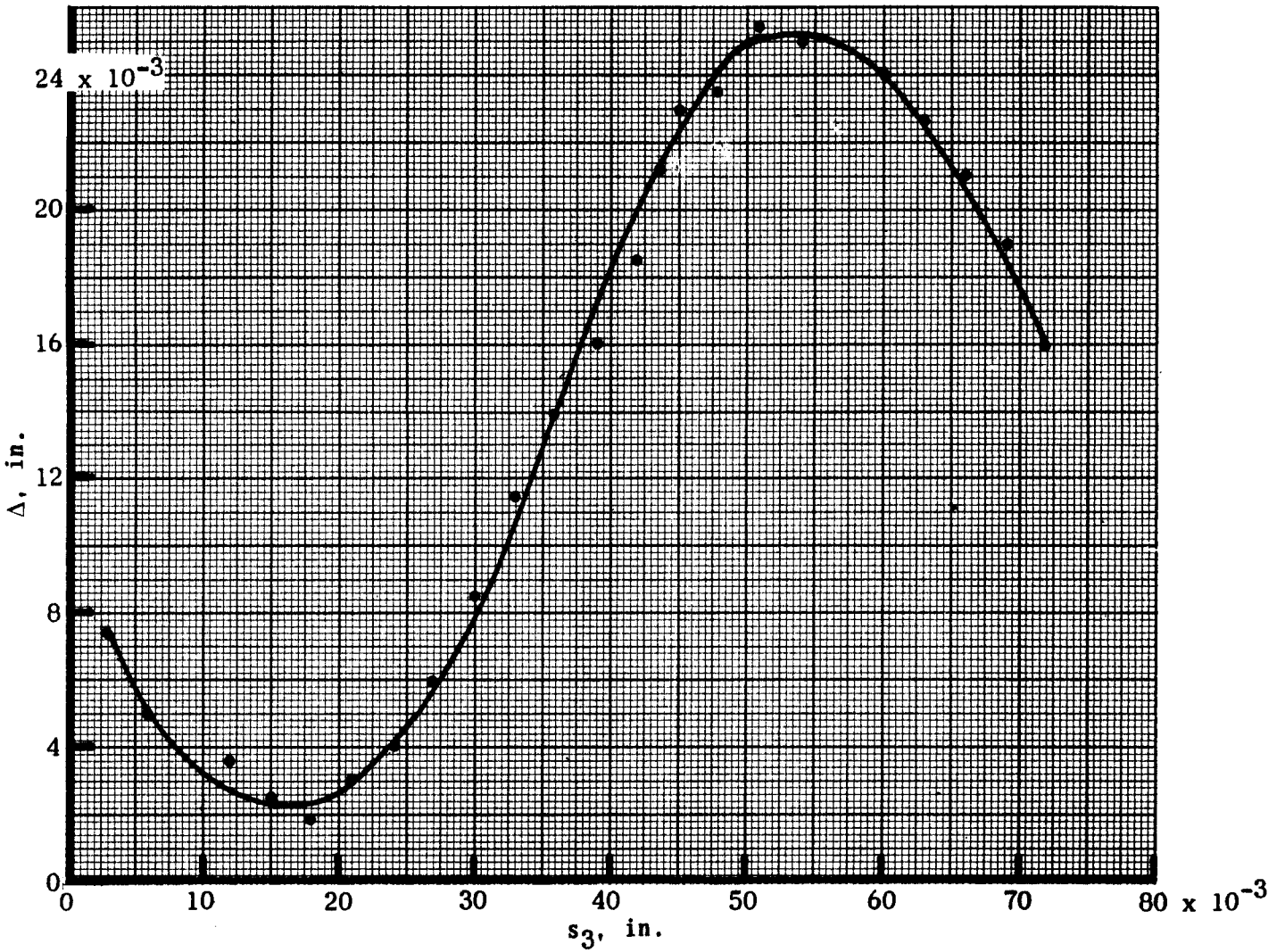

Figure 9.- Experimental curve of Δ necessary to restore resonance vs. position of dielectric sheet for polystyrene (s_1 = 2.010 in.).

half-wavelengths. The results obtained using this method for the various materials with different thicknesses and surface finishes are tabulated in Table II.

In order to determine the variation of ϵ as a function of frequency, measurements were made within the range of 59.0 to 62.2 GHz. The results obtained are shown in Table III. Plots of dielectric constant versus frequency for the different materials are shown in Figure 10. It is seen that the dielectric constant for polystyrene and plexiglas remains approximately the same in that frequency range. However the dielectric constant for teflon seems to be somewhat lower at higher frequencies. Since the variations in the dielectric constant in this frequency range are very gradual, the frequency range should be extended much higher to actually verify the changes in dielectric constant.

Using data available at lower frequencies,[19,20,21] plots of dielectric constant and loss tangent versus frequency were drawn and are shown in Figures 11, 12, and 13. There seems to be a transition in the microwave region which continues into the millimeter region. Before forming any conclusions,

---

[19] Arthur R. Von Hippel, Dielectric Materials and Applications, (The Technology Press of M. I. T., 1954), pp. 332-335.

[20] B. W. Hakki; and P. D. Coleman, "A Dielectric Resonator Method of Measuring Inductive Capacities in the Millimeter Range." IRE Transactions on Microwave Theory and Techniques, 8"408, July 1960.

[21] W. Culshaw; and M. V. Anderson, op. cit. p. 29.

TABLE II

DIELECTRIC CONSTANTS FOR VARIOUS MATERIALS OF SEVERAL THICKNESSES AND VARIOUS SURFACE FINISHES AT CONSTANT TEMPERATURE USING 2nd METHOD

TEFLON - 25 °C

Thickness / Surface Finish	1.0221±.005 / 32	1.0922±.001 / 16	1.6370±.001 / 16	2.0877±.005 / 32
Dielectric Constant	2.055	2.048	2.050	2.057
Frequency MHz	61,452.551	61,452.551	61,452.551	61,452.551

POLYSTYRENE - 25 °C

Thickness / Surface Finish	0.9852±.001 / 32	1.0123±.002 / 64	1.4734±.001 / 32	2.0100±.002 / 130
Dielectric Constant	2.534	2.530	2.528	2.532
Frequency MHz	61,452.551	61,452.551	61,452.551	61,452.551

PLEXIGLAS - 25 °C

Thickness / Surface Finish	0.1235±.002 / 8	0.1831±.002 / 8	0.3718±.003 / 8
Dielectric Constant	----------	2.586	2.605
Frequency MHz	----------	61,452.551	61,452.551

TABLE III

DIELECTRIC CONSTANTS FOR VARIOUS MATERIALS AT DIFFERENT FREQUENCIES AND CONSTANT TEMPERATURE (25 ^{o}C)

Frequency MHz	Dielectric Constant Teflon (1.0922 in.)	Dielectric Constant Polystyrene (1.0123 in.)	Dielectric Constant Plexiglas (0.1235 in.)
62,139.843	2.005	2.533	2.576
61,539.994	2.020	2.535	2.569
60,943.657	2.055	2.534	2.586
60,278.047	2.058	2.530	2.576
59,562.875	2.060	2.534	2.576
59,315.299	2.062	2.537	2.582
59,023.320	2.056	2.533	2.571

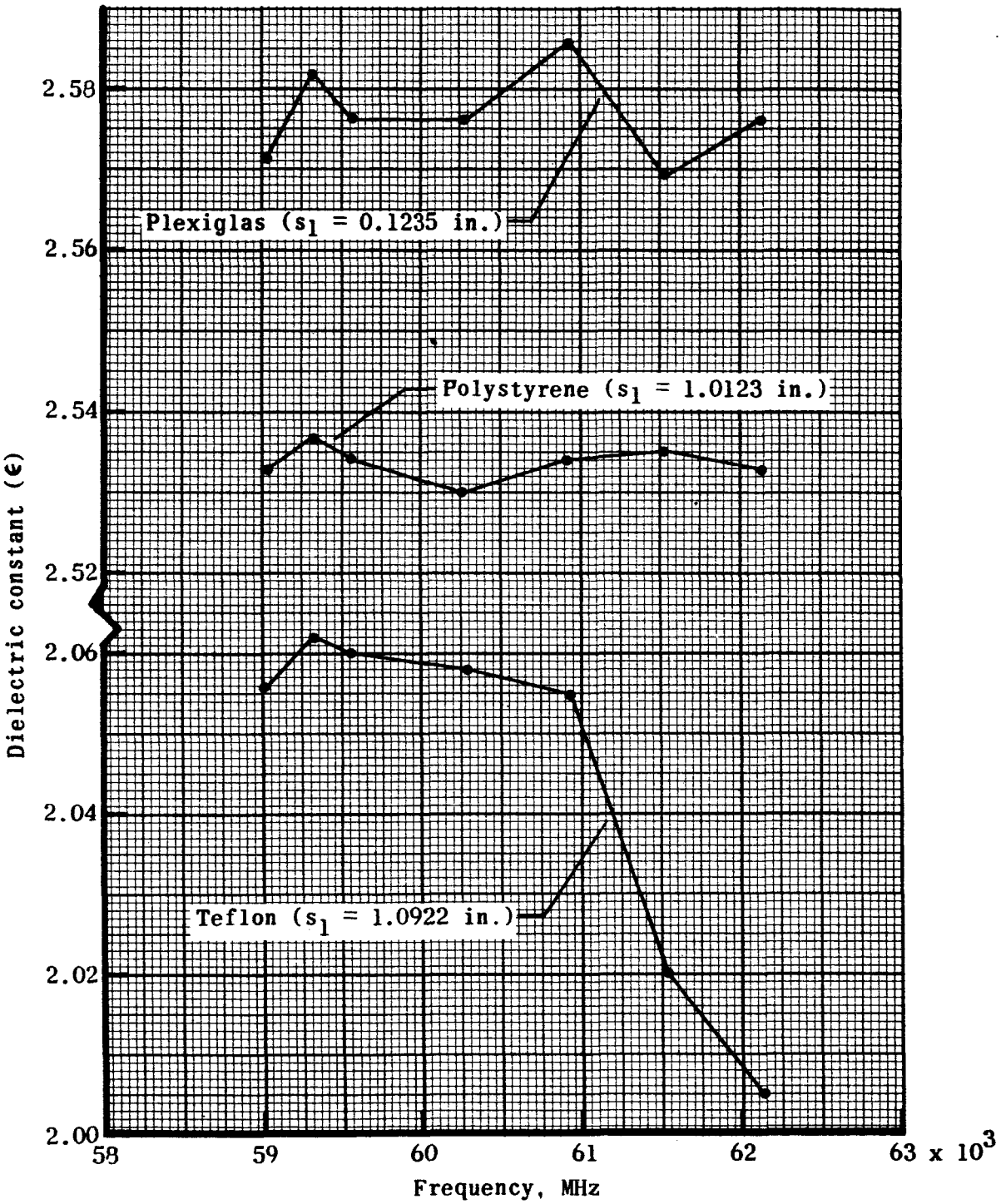

Figure 10.- Dielectric constant vs. frequency at 25° C.

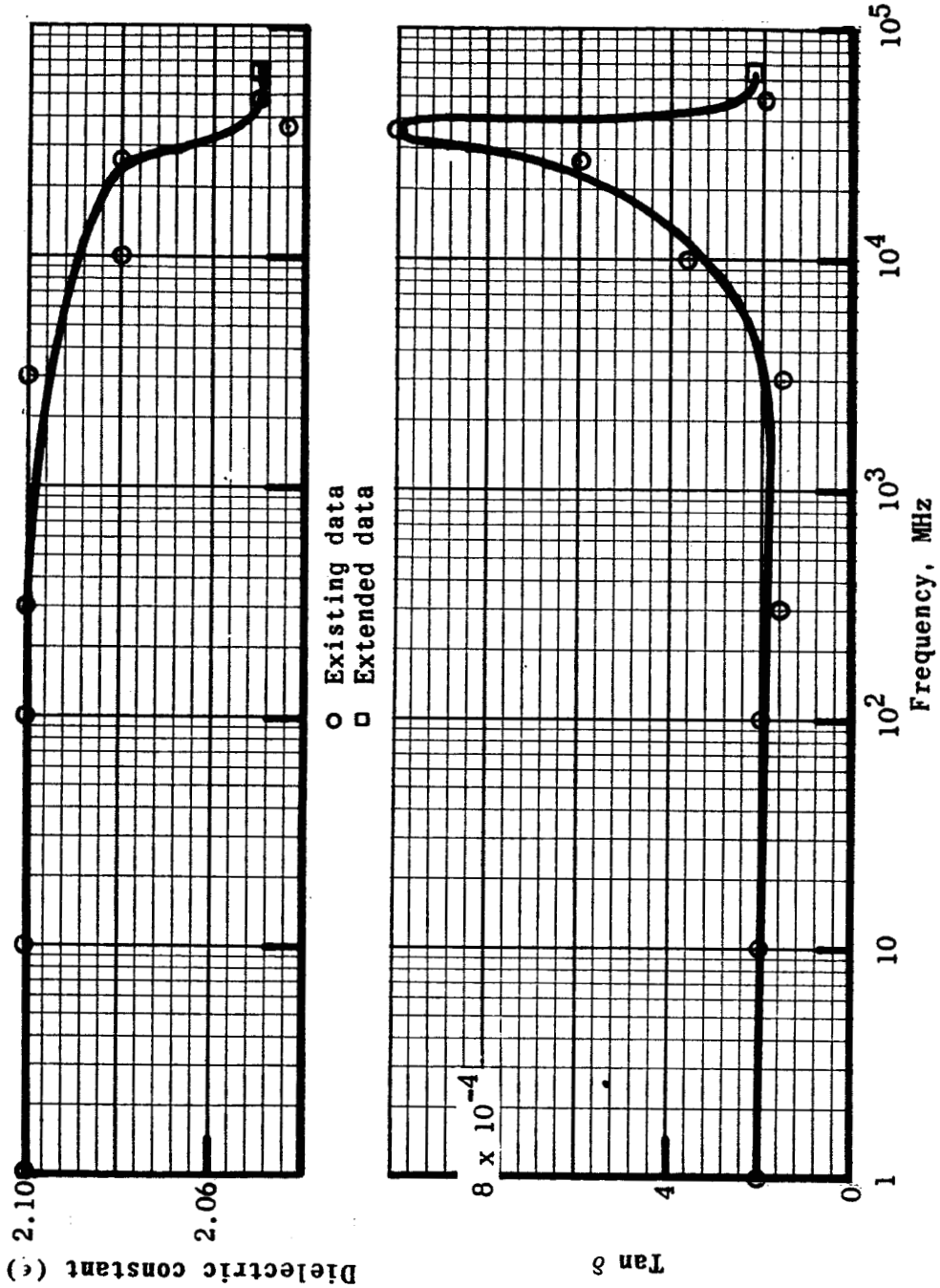

Figure 11.- Dielectric constant and loss tangent vs. frequency for teflon.

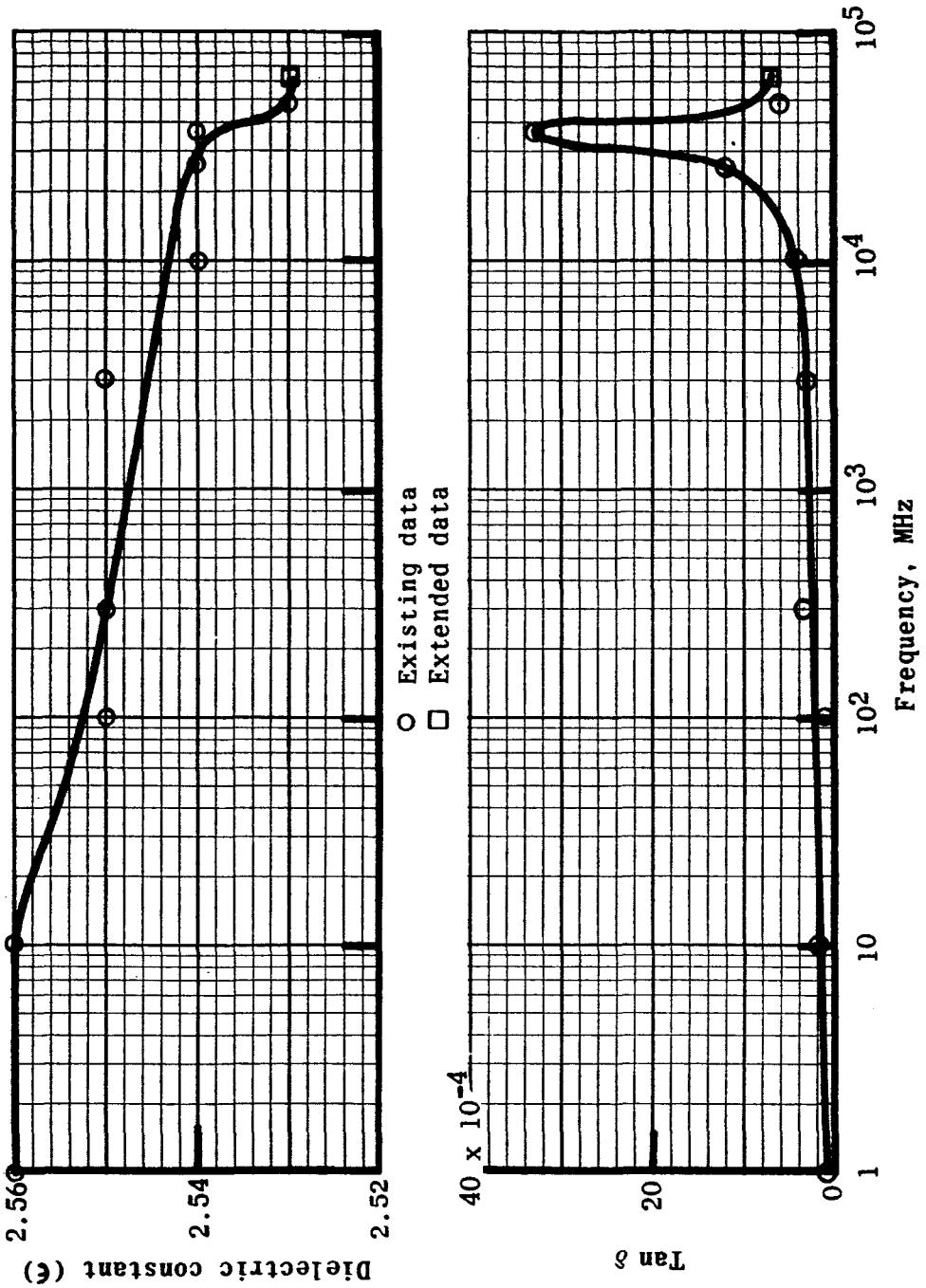

Figure 12.- Dielectric constant and loss tangent vs. frequency for polystyrene.

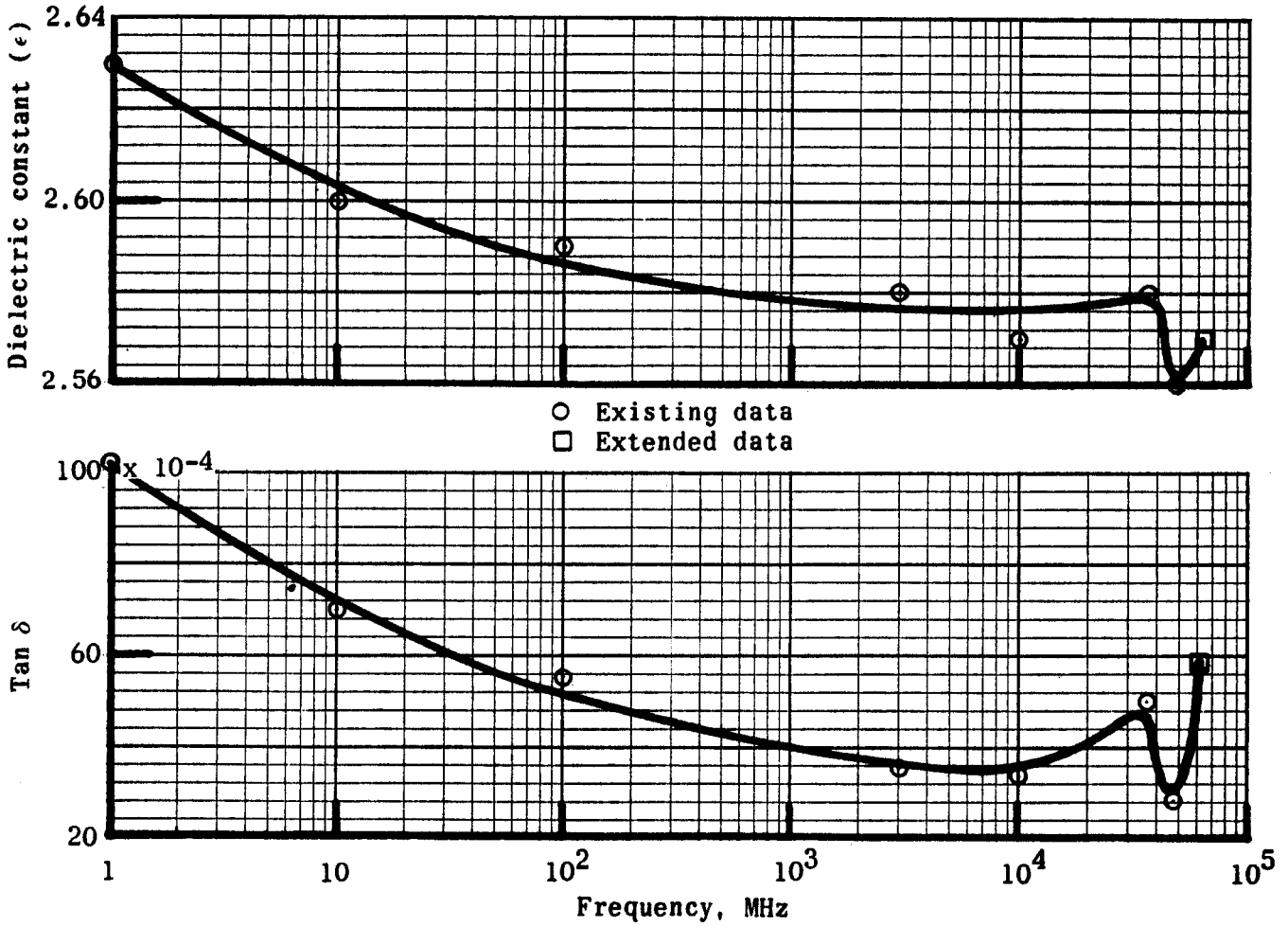

Figure 13.- Dielectric constant and loss tangent vs. frequency for plexiglas.

it must be pointed out that the data available at lower microwave frequencies were obtained by different experimenters using slightly different homogenuities in the same type of material. There could be enough difference in the homogenuity of the same materials used by the different authors to affect, to some extent, the shape of the curves. The only way to form any positive conclusions would be to use the same slabs throughout the frequency range of comparison. However, there is enough similarity between these curves and the one in Figure 1, to suspect such a transition.

A theoretical prediction of the transition period is the relaxation time[22]. The real and imaginary parts of the dielectric constant using Debye's equations are given by

$$\epsilon'(w) = \epsilon_{ea} + \frac{\epsilon_s - \epsilon_{ea}}{1+w^2\tau^2} \tag{49}$$

$$\epsilon''(w) = \epsilon_s - \epsilon_{ea} \quad \frac{w\tau}{1+w^2\tau^2} \tag{50}$$

Where: $\epsilon^* = \epsilon' - j\epsilon''$ - complex dielectric constant
ϵ_s - static dielectric constant
ϵ_{ea} - instantaneous dielectric constant
τ - relaxation time

The plots of ϵ' and ϵ'' as a function of $w\tau$ using the above equations are shown in Figure 14. It is observed that the dielectric loss, which is proportional to ϵ'', is maximum when $w = 1/\tau$.

---

[22] A. J. Decker, op. cit. pp. 150-152.

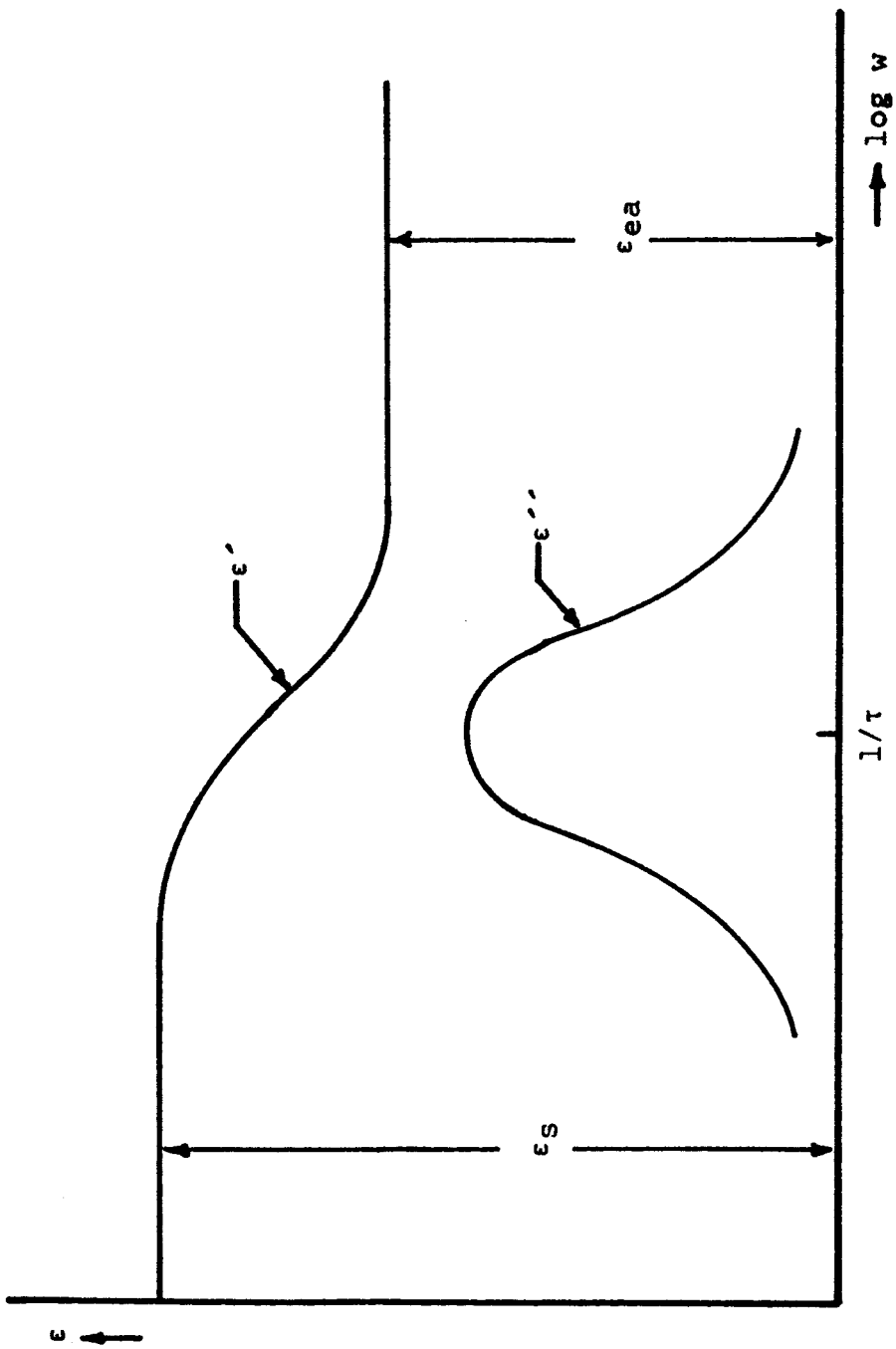

Figure 14.- Real and imaginary parts of complex dielectric constant of dielectric with a single relaxation time.

When the operating angular frequency is less than $1/\tau$, the real part of the dielectric constant ϵ' is equal to the static dielectric constant ϵ_s. For angular frequencies appreciably greater than $1/\tau$, ϵ' approaches the instantaneous dielectric constant ϵ_{ea}.

The relaxation times calculated using the experimental results with equations (49) and (50) for the different materials are $\approx 2.34 \times 10^{-10}$ sec. for teflon, $\approx 2.42 \times 10^{-10}$ sec. for polystyrene and $\approx 1.10 \times 10^{-10}$ sec. for plexiglas. The experimental operating angular frequency was larger than $1/\tau$ for each one of the above values. This is an indication that the region of maximum dielectric loss has been passed which in another way verifies the plots of Figures 11, 12, and possibly 13.

The dielectric constant for dipolar substances is a function of temperature[23]. As the temperature is increased the dielectric constant decreases because of the increased thermal motion and the change of the density of the material. The results obtained from the test are shown in Table IV, and plots of dielectric constant versus temperature for each material are shown in Figure 15. The reduction of dielectric constant at higher temperatures is indicated. Extension of the temperature range for much higher and lower values would better verify these conclusions.

---

[23] Charles P. Smyth, Dielectric Behavior and Structure (New York: McGraw-Hill Book Company, Inc., 1955), pp. 132-201.

TABLE IV

DIELECTRIC CONSTANTS OF DIFFERENT MATERIALS FOR VARIOUS TEMPERATURES AND CONSTANT FREQUENCY

Temperature ^{o}C	Frequency MHz	Dielectric Constant		
		Teflon 1.0922 in.	Polystyrene 1.0123 in.	Plexiglas 0.1235 in.
-8	61,242.103	2.048	2.545	2.626
8	61,242.103	2.047	2.545	2.607
24	61,242.103	2.036	2.538	2.596
32	61,242.103	2.027	2.531	2.574
46	61,242.103	2.020	2.527	2.578
65	61,242.103	2.014	2.520	2.569
77	61,242.103	2.010	2.515	2.554

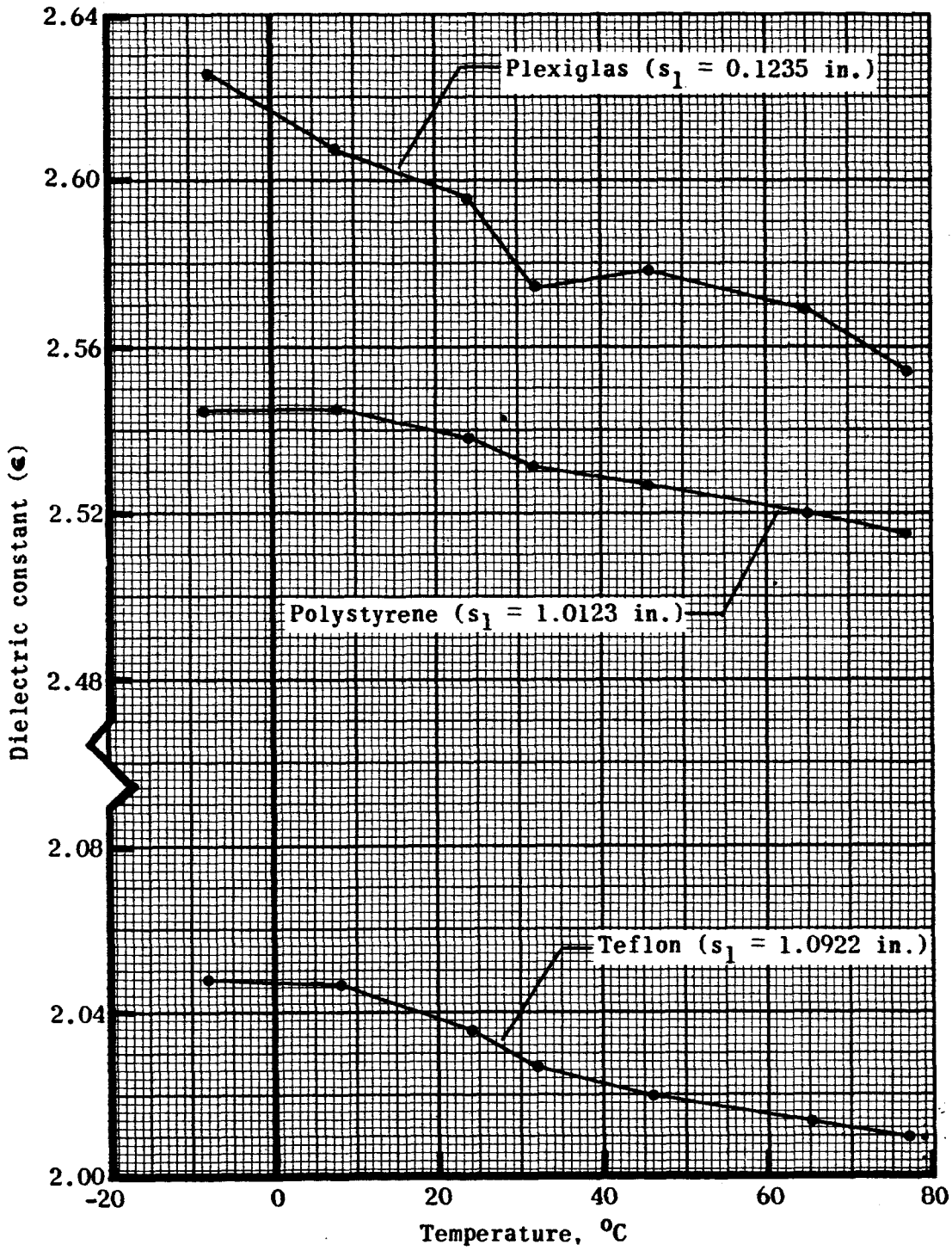

Figure 15.- Dielectric constant vs. temperature at 61,242.103 MHz.

Loss Tangent Measurements

Before any measurements of loss tangent were made, experimental curves of Q versus plate separation were plotted, and they are shown in Figure 16. These curves closely resemble the predicted shapes.[24] No data could be taken for plate separations less than about five inches due to the presence of the middle frame.

It is seen that a linear relation exists between Q and plate separation with air for separations up to about seven inches. This is an indication of the small effect of the diffraction losses in that region. As the plate separation is increased further, the diffraction losses become noticeable and the experimental curve is flattened. The curves with the different dielectrics between the plates begin to flatten at smaller plate separations. This indicates that diffraction losses become noticeable at shorter plate separations possibly due to the surface imperfections of the dielectrics. The Q's measured at closer spacings should represent more dependable results. The cavity response with each material between its plates is shown in Figure 17.

To make loss tangent measurements, slabs whose thicknesses are multiples of half-wavelengths were used. This was done to simplify the calculations. The maximum Q with the dielectric between the plates must be determined for each slab. This can be done by plotting Q as a function of plate position using equation (45). An experimental curve is shown in Figure 18. Once Q_{tmax} is determined, the Q without the slab

---

[24] See Appendix I.

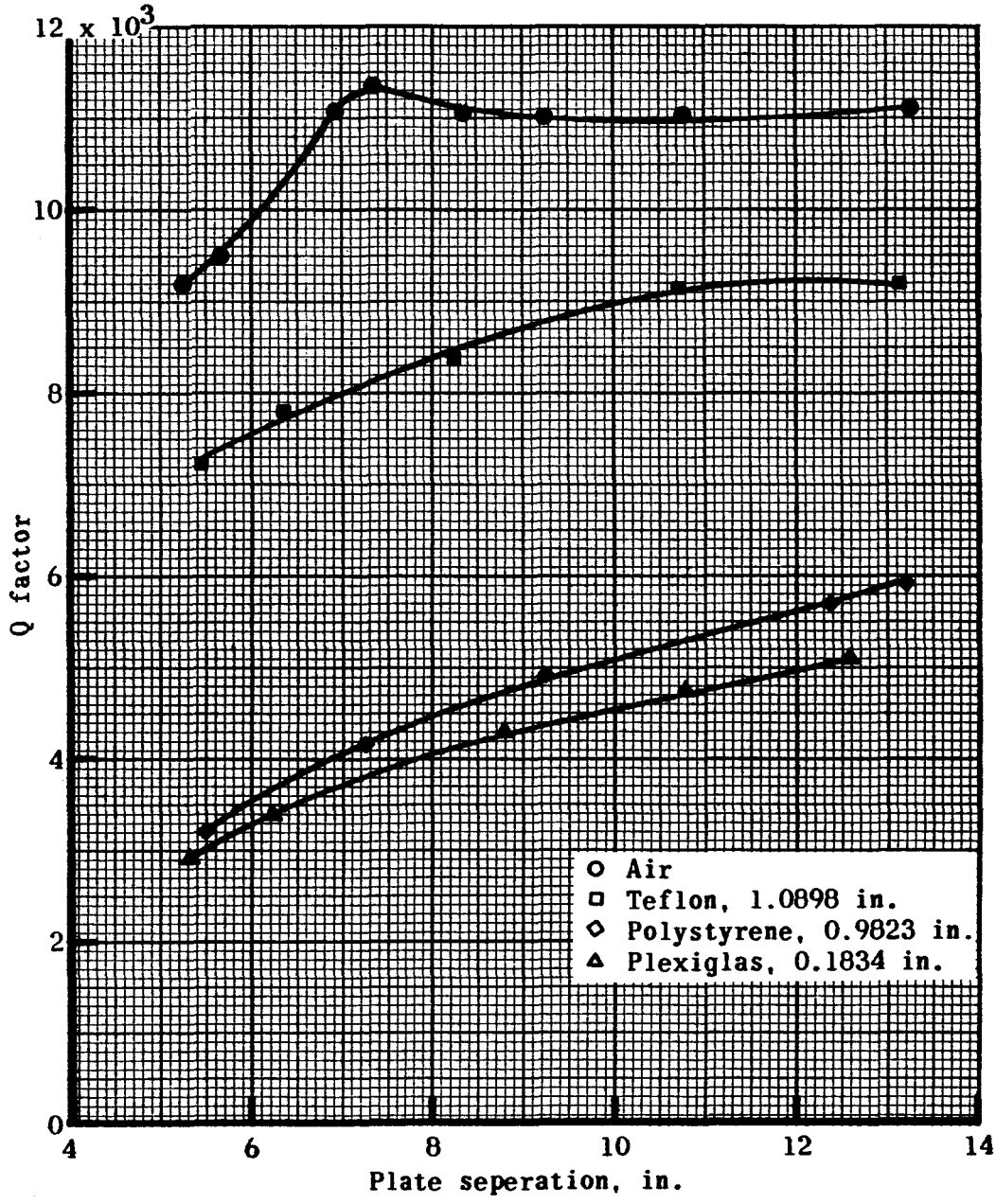

Figure 16.- Q factor vs plate separation for air and other dielectric sheets.

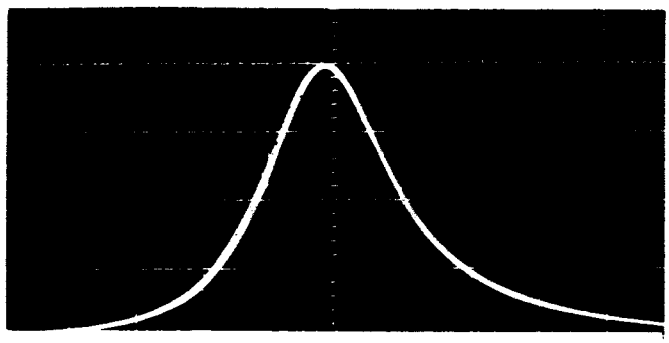

(a) Teflon. (1.0922 in.). Q = 7,042.

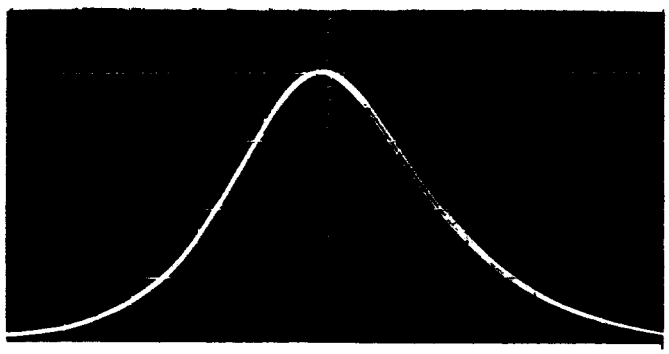

(b) Polystyrene. (1.0123). Q = 4,049.

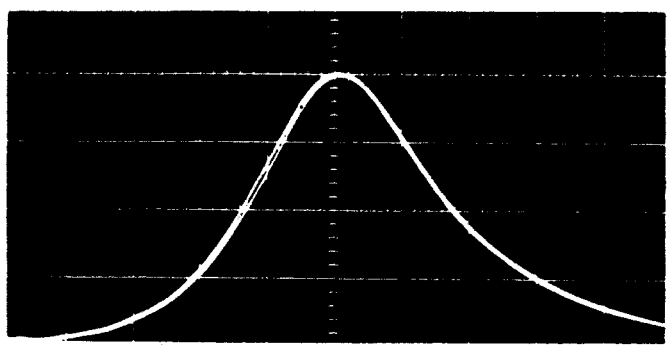

(c) Plexiglas. (0.1235 in.). Q = 4,407.

Figure 17.- Cavity response for different materials at 61,398.163 MHz.

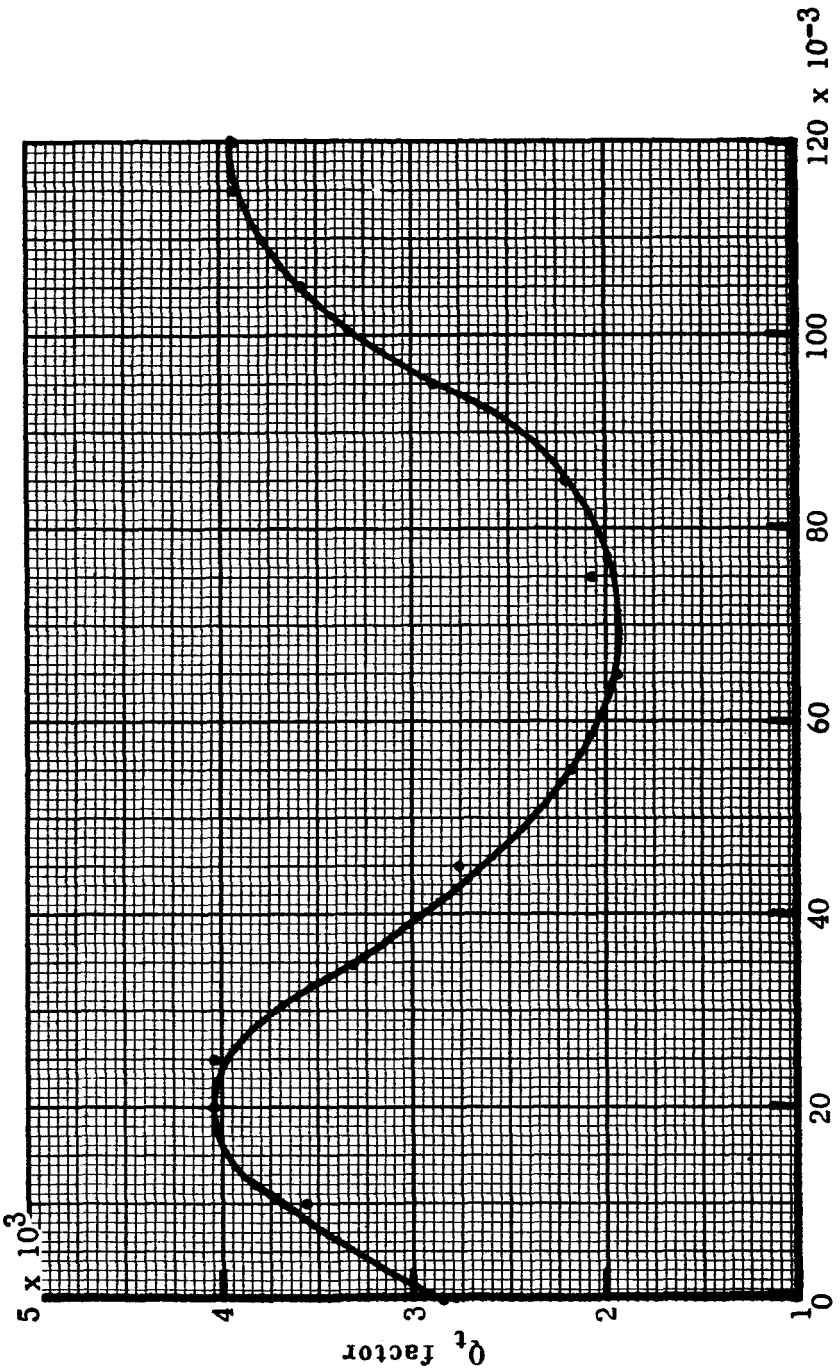

Figure 18.- Q_t factor as a function of relative position of dielectric sheet for plexiglas (s_1 = 0.1831 in.).

must be measured with the same position and spacing between the plates. These two values along with the slab thickness and plate separations can be used with equation (46) to determine tanδ. The assumption made in these measurements is that the diffraction losses with and without the slab are the same. This is not true, but the difference at close plate separations may be small and can be neglected.

The tanδ values vary as a function of plate separation because of the increase of diffraction losses for separations greater than approximately the diameter of the plates. Therefore, the most accurate data will be for plate separations up to approximately the diameter of the plates.

The results obtained from the measurements are shown in Table V. It is seen that the values of teflon for larger plate spacings are somewhat greater. This can be attributed to the increase of diffraction losses with increasing plate separation.

TABLE V

LOSS TANGENTS FOR VARIOUS MATERIALS OF SEVERAL THICKNESSES AND VARIOUS SURFACE FINISHES AT CONSTANT TEMPERATURE (25 °C)

Material	Thickness(in.) Surface Finish	Frequency MHz	tanδ x10^4 d≈4.8 in.	tanδ x10^4 d≈5.5 in.	tanδ x10^4 d≈6.5 in.
Teflon	1.0221±.005 32	60,539.235	2.34	1.82	2.15
	1.0922±.001 16	60,319.345	2.39	2.21	2.75
	1.6370±.001 16	60,449.572	----	2.27	3.05
Polystyrene	0.9852±.001 32	60,246.897	----	6.98	7.05
	1.0123±.002 64	58,677.897	----	9.41	9.72
	1.4734±.001 32	60,418.072	----	7.16	7.15
Plexiglas	0.1235±.002 8	59,562.875	---=	59.45	59.09
	0.1831±.002 8	60,065.323	----	59.14	58.87

CHAPTER V

CONCLUSIONS

The results of the investigation verified the use of the Fabry-Perot interferometer as an effective instrument for the measurements of dielectric constants and loss tangents at millimeter wave frequencies. Increasing the frequency range will not limit its application.

The two methods used for the measurements of dielectric constants must be carefully examined for accurate prediction of the results. The use of the first method suggested that there are many Δ's which will restore resonance and each can be used with equation (32) as discussed in Chapter III. It was concluded from the use of slabs of several thicknesses, there will be found only one value of k which will be the same for each thickness. Otherwise, it seems impossible to determine the correct value of k unless its approximate value is previously known.

To use the second method, an iterative process must be applied in determining the correct value of k. Again, there are many values of k which will satisfy equations (28) and (29). The only way to determine the correct values of k would be to use different thickness slabs of the same material, find the different roots and compare the k's. As in the first method, there should be only one value of k which will be the same for each thickness. It is suggested that the range of k be determined, if possible, by the use of the first method before the second method is used. A computer program was used with the second method and is highly recommended for convenience and accuracy.

For frequency stabilities of 1 part in 10^4 or better and for dimension measurements within 0.001 inches, the values of the dielectric constants obtained using both methods are within one per cent or better. As the slab thickness is increased, the accuracy of the results is increased. Therefore, the values of ϵ for teflon and polystyrene should be much more accurate. Frequency stabilities stated above are compatible with the dimension measurements accuracy. The variable surface finishes and tolerances which were used in our measurements seem to have no effect on the values of ϵ, at least within the accuracy stated above.

The dielectric constant is a function of frequency and temperature. Existing data at lower frequencies and our results seem to indicate a transition in the microwave region. As the temperature is increased, the dielectric constant seems to decrease. Extension of the frequency range to much higher frequencies and the change of temperature to much higher and lower values should more accurately validate these conclusions.

The accuracy of the loss tangent measurements is based upon the accuracy of the Q's. In general, it was possible to measure the half-power bandwidth points repeatly to about $\pm$ 2 per cent. For such accuracy in frequency measurements, the values of tanδ are within about $\pm$ 15 per cent for teflon and about $\pm$ 6 per cent for polystyrene and plexiglas. The effect of the diffraction losses are noticeable at the lower loss materials such as teflon. With increasing plate separation, the tanδ values for teflon are a little higher which is an indication

of the effect of diffraction losses. The surface finishes and tolerances should affect the Q measurements. However, for the surface finishes, tolerances, frequency accuracy measurements and plate separations used in the tests, no noticeable differences in the results could be detected. The more dependable values should be for closer spacings.

BIBLIOGRAPHY

BIBLIOGRAPHY

1. Boyd, G. D.; and Gordon, J. P., "Confocal Multimode Resonator for Millimeter Through Optical Wavelength Masers", Bell System Technical Journal, 40:490-491, March, 1961.

2. Brekhovikish, Leonid M., Waves in Layered Media, New York: Academic Press, Inc., 1960.

3. Culshaw, W., "High Resolution Millimeter Wave Fabry-Perot Interferometer", United States Department of Commerce, National Bureau of Standards, Boulder, Colo., NBS Report 6039.

4. Culshaw, W., "Resonators for Millimeter and Submillimeter Wavelengths", IRE Transactions on Microwave Theory and Techniques, 9:135-144, March 1961.

5. Culshaw, W.; and Anderson, M. V., "Measurements of Dielectric Constants and Losses with a Millimeter Wave Fabry-Perot Interferometer", United States Department of Commerce, Boulder, Colo., NBS Report 6786, July 19, 1961.

6. Decker, A. J., Solid State Physics, New York: Prentice Hall, Inc., 1946.

7. Hakki, B. W.; and Coleman, P. D., "A Dielectric Resonator Method of Measuring Inductive Capacities in the Millimeter Range", IRE Transactions on Microwave Theory and Techniques, 8:408, July 1960.

8. Kraus, John D., Electromagnetics, New York: McGraw-Hill Book Company, Inc., 1953.

9. Lamont, H. R. L., "Theory of Resonance in Microwave Transmission Lines with Discontinuous Dielectrics", Philosophical Magazine, 29:521-531, June 1940.

10. Montogomery, Carol G., Techniques of Microwave Measurements, New York: McGraw-Hill Book Company, Inc., 1947.

11. Smyth, Charles P., Dielectric Behavior and Structure, New York: McGraw-Hill Book Company, Inc., 1955.

12. Stratton, Julius A., Electromagnetic Theory, New York: McGraw-Hill Book Company, Inc., 1941.

13. Von Hippel, Arthur R., Dielectric Materials and Applications, The Technology Press of M. I. T., 1954.

14. Zimmerer, R. W.; Anderson, M. V.; Strine, G. L.; and Beers, Y., "Millimeter Wavelength Resonant Structures", IEEE Transactions on Microwave Theory and Techniques, 11: 142-149, March 1963.

APPENDICES

APPENDIX I

Fabry-Perot Resonant Cavity

The photograph of the basic structure of a flat-plate Fabry-Perot resonant cavity is shown in Figure 19. The inside faces of the reflector plates are coated with a thin film of gold which has a high reflection coefficient.

The Q (quality factor) of the cavity is a function of plate separation, diffraction losses, and reflection losses. The side wall losses which are present in cavities of lower microwave frequencies have been eliminated by the absence of any side walls. However, diffraction losses have been introduced which result from the finite aperature of the reflector plates and from the imperfection in their flatness. Any misalignment of the plates from parallelism will increase diffraction losses and reduce the Q. Reflection losses are present because of the absorption in the reflector plates and transmission through them. Reflection losses are a function of the resistivity of the material employed and the transmission coefficient of the plates. Diffraction losses can be controlled by the use of the appropriate size of reflector plates and plate separation. The Q of the Fabry-Perot resonator as a function of mirror separation is given[25] by

$$Q = 2\pi d/\gamma\lambda \qquad \text{(I-1)}$$

---

[25] G. D. Boyd and J. P. Gordon, "Confocal Multimode Resonator for Millimeter Through Optical Wavelength Masers", Bell System Technical Journal. 40:490-481, March 1961.

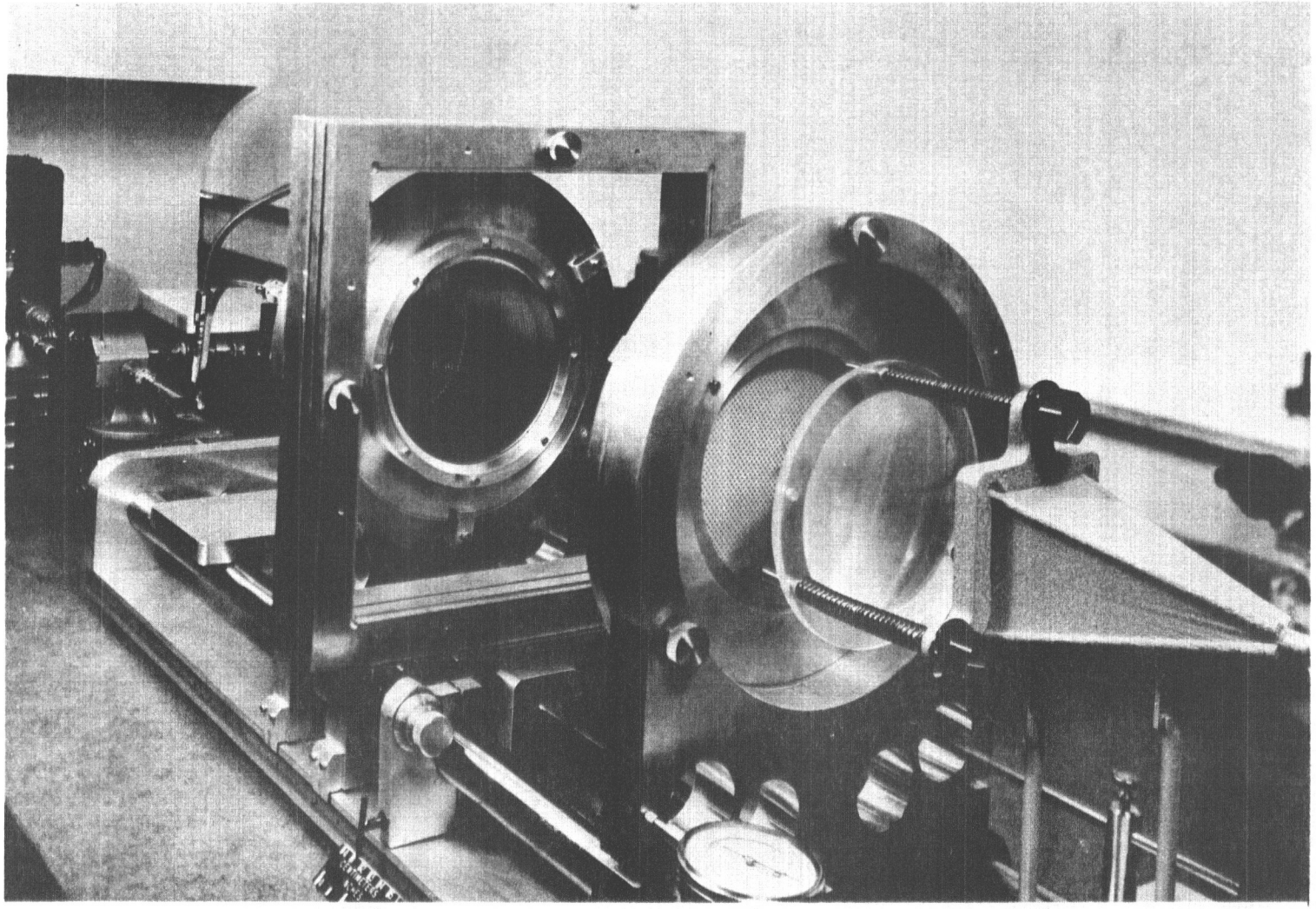

Figure 19.- Structure of a flat-plate Fabry-Perot resonant cavity.

Where: d = distance between reflecting plates
λ = operating wavelength
γ = the sum of reflection and diffraction losses

It would seem valid that for a given value of reflection and diffraction losses the Q would vary linearly as the plate separation, and conceivably the larger the plate separation the higher the Q. However, such an assumption would not be valid since diffraction and reflection losses are functions of plate separation. As the plate separation increases the reflection losses decrease and the diffraction losses increase. Thus, at some point, the combination of reflection and diffraction losses along with the plate separation would be such that a maximum Q is achieved. As the plate separation is increased beyond that point the value of Q will begin to decrease. Figure 20 demonstrates how the theoretical and experimental values of Q vs. plate separation v a r y. There should be a linear relation up to a certain point, and this would indicate that the sum of diffraction and reflection losses is approximately constant. As the plate separation is increased further the sum of the diffraction and reflection losses does not stay constant but varies resulting in the bending of the curve.

When a dielectric is inserted between the plates additional losses are introduced. The propagation losses through the medium must be accounted for and would vary as the thickness of the sample. Thus an additional term must be considered in deciding on the value of γ. It must also be remembered that additional diffraction losses could result from the insertion of the dielectric between the plates from the imperfections of the surfaces of the sample. The experimental values

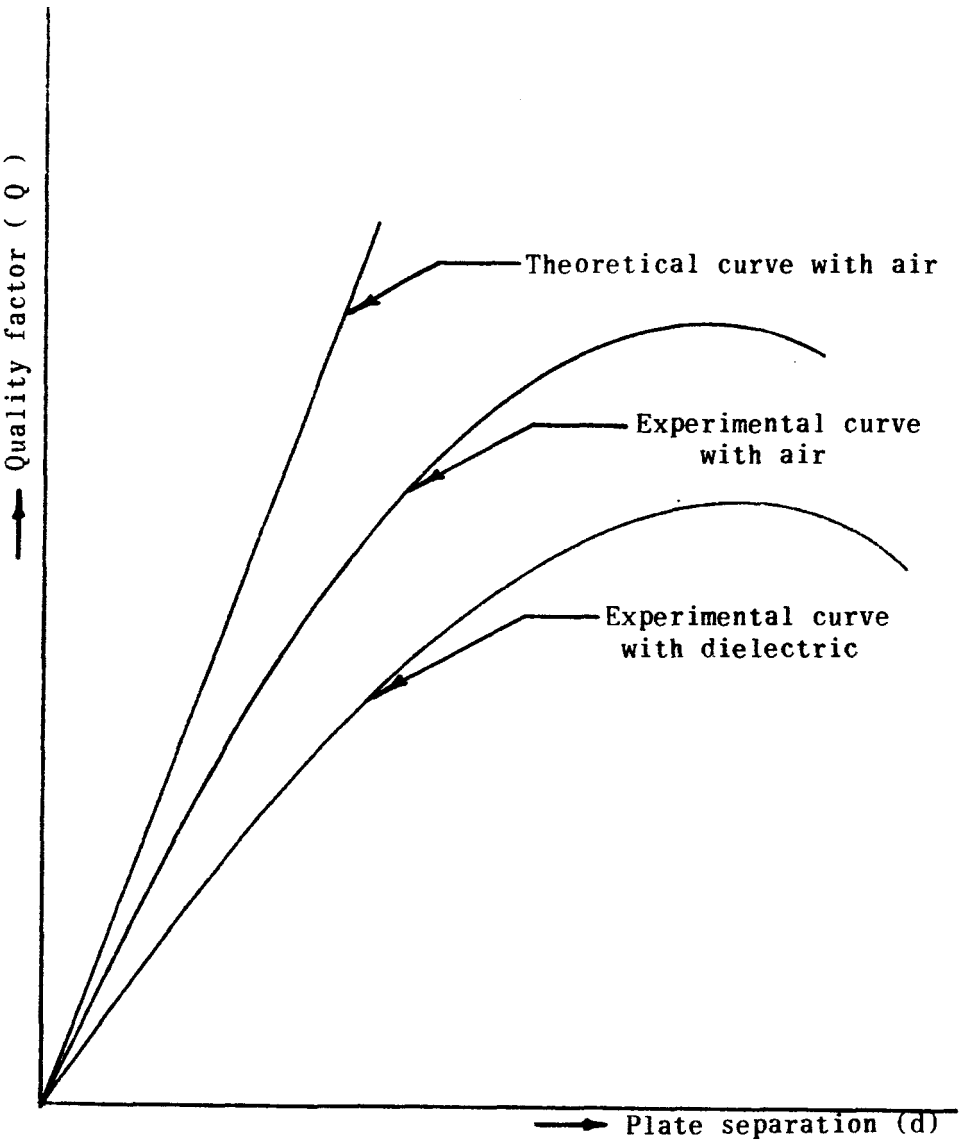

Figure 20.- Quality factor vs. plate separation for flat-plate resonant cavity.

of Q when the dielectric material is inserted between the plates should be lower than the corresponding values without the dielectric because of the increase in the value of γ due to the presence of the sample, as discussed above.

Operating Principle

The resonant cavity which was introduced above can be thought of as being an interference lightfilter[26] which is used extensively in the field of optics. When the plate separation is an integral number of a half-wavelength ($d = \lambda/2, \lambda, 3\lambda/2$, ----), complete reflection occurs, and the electric field intensity at the boundary will be zero, assuming that the reflecting surface is a perfect conductor. Hence, the metallic surface of the reflecting plate will absorb no energy from the electromagnetic wave. Practically, such a surface can not be constructed, but surfaces with reflection coefficients close to unity can be achieved. Since an ideal voltage node can not be attained, wave absorption in the lightfilter is due to the ohmic losses of currents induced in the metallic surfaces.

When the plate separation is equal to $d = \lambda/4, 3\lambda/4, 5\lambda/4$ ------, minimum reflection will occur. If the metallic surface of one reflecting plate is located at a node of the electric field, then the surface of the other reflecting plate will be at an antinode and the absorption of the electromagnetic wave by the plates of the lightfilter will be

---

[26] Leonid M. Brekhovikish, Waves in Layered Media (New York: Academic Press Inc., 1960), pp. 148-151.

maximum. The above statements concerning the transmission of the lightfilter can be verified mathematically by considering the resonant cavity of the interferometer, Figure 21, and apply the principle of multiple reflections assuming plane waves.

For simplification of notation, we assume that the transmission coefficients $t_{12} = t_{21} = t_{23} = t$ and reflection coefficients $\rho_1 = \rho_2 = \rho_3 = \rho$. The principle of operation is the same and is best illustrated by the more simplified notation. The fields in the various regions can then be calculated. Thus, in region no. 1 the field E_1 can be expressed by

$$E_1 = E_o \rho + E_o t^2 \rho\, e^{-j2\beta d} + E_o t^2 \rho^3 e^{-j4\beta d} + E_o t^2 \rho^5 e^{-j6\beta d} + \text{-----}$$

$$E_1 = \rho E_o \left[1 + t^2 e^{-j2\beta d}\left(1 + \rho^2 e^{-j2\beta d} + \rho^4 e^{-j4\beta d} + \text{-----}\right)\right]$$

$$E_1 = \rho E_o \left\{1 + t^2 e^{-j2\beta d}\left[\frac{1}{1 - \rho^2 e^{-j2\beta d}}\right]\right\}$$

$$\frac{E_1}{E_o} = \frac{\rho\left[1 + \left(t^2 - \rho^2\right) e^{-j2\beta d}\right]}{1 - \rho^2 e^{-j2\beta d}} \qquad \text{(I-2)}$$

The ratio of $\left|E_1/E_o\right|$ defines the total reflection coefficient of the resonant cavity. Similarly, the field in region no. 2 is found to be

$$E_2 = E_o t\, e^{-j\beta x} + E_o\, t\rho e^{-j\beta(2d-x)} + E_o\, t\rho^2\, e^{-j\beta(2d+x)}$$

$$+ E_o\, t\rho^3\, e^{-j\beta(4d-x)} + E_o\, t\rho^4\, e^{-j\beta(4d+x)}$$

$$E_2 = E_o\, t\, e^{-j\beta x}\left[1 + \rho\, e^{-j2\beta(d-x)} + \rho^2\, e^{-j2\beta d} + \rho^3\, e^{-j2\beta(2d-x)} + \text{-----}\right]$$

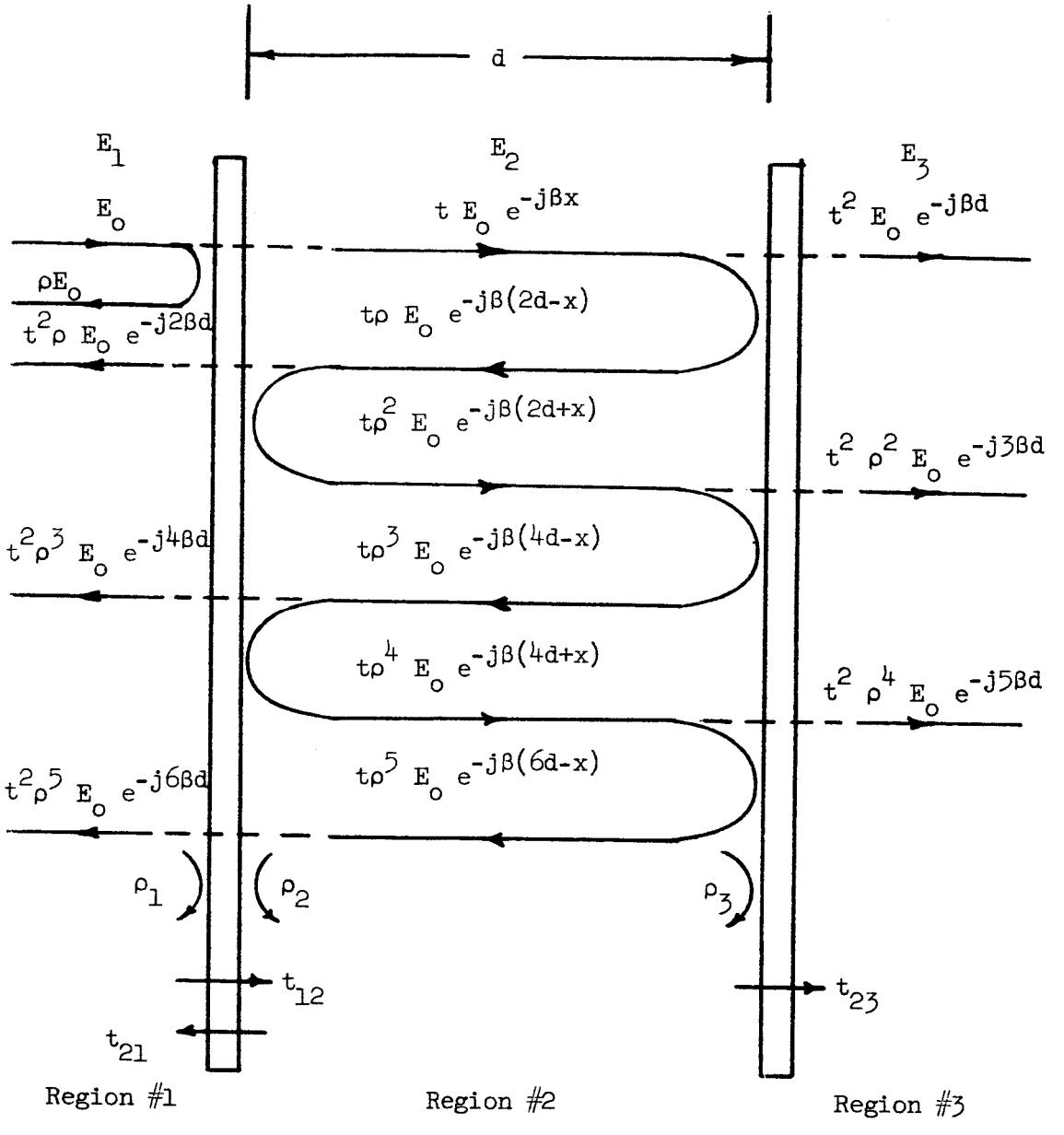

Figure 21.- Flat-plate resonant cavity.

$$E_2 = E_o\, t\, e^{-j\beta x}\left[1 + \rho\, e^{-j2\beta(d-x)}\right]\left[1 + \rho^2\, e^{-j2\beta d} + \rho^4\, e^{-j4\beta d} + \text{-----}\right]$$

$$\frac{E_2}{E_o} = \frac{t\, e^{-j\beta x}\left[1 + \rho\, e^{-j2\beta(d-x)}\right]}{1 - \rho^2\, e^{-j2\beta d}} \qquad \text{(I-3)}$$

The field in region no. 3 is given by

$$E_3 = E_o\, t^2\, e^{-j\beta d} + E_o\, t^2\rho^2\, e^{-j3\beta d} + E_o\, t^2\rho^4\, e^{-j5\beta d} + \text{-----}$$

$$E_3 = E_o\, t^2\, e^{-j\beta d}\left[1 + \rho^2\, e^{-j2\beta d} + \rho^4\, e^{-j4\beta d} + \text{-----}\right]$$

$$\frac{E_3}{E_o} = \frac{t^2\, e^{-j\beta d}}{1 - \rho^2\, e^{-j2\beta d}} \qquad \text{(I-4)}$$

The ratio of $\left|E_3/E_o\right|$ defines the transmission coefficient of the entire resonant cavity.

To find the optimum spacing for maximum transmission, equation (I-4) is differentiated with respect to βd and then set equal to zero. Thus,

$$1 + \rho^2\, e^{-j2\beta d} = 0$$

$$\beta d = \frac{n\pi}{2} \qquad n = 1, 2, 3, 4, \text{-----} \qquad \text{(I-5)}$$

Maximum transmission occurs when

$$\beta d = \frac{n\pi}{2} \qquad n = 2, 4, 6, \text{-----} \tag{I-6}$$

or

$$d = \lambda/2, \lambda, 3\lambda/2, \text{-----} \tag{I-7}$$

Minimum transmission occurs when

$$\beta d = \frac{n\pi}{2} \qquad n = 1, 3, 5, \text{-----} \tag{I-8}$$

or

$$d = \lambda/4, 3\lambda/4, 5\lambda/4, \text{-----} \tag{I-9}$$

The magnetic fields in the three regions can be calculated using the same procedure as for the electric fields, and they are given by

$$H_1 = -\frac{E_o \rho \left[1 + e^{-j2\beta d}\right]}{Z_o \left[1 - \rho^2 e^{-j2\beta d}\right]} \tag{I-10}$$

$$H_2 = \frac{E_o t e^{-j\beta x} \left[1 - p e^{-j2\beta(d-x)}\right]}{Z_o \left[1 - \rho^2 e^{-j2\beta d}\right]} \tag{I-11}$$

$$H_3 = \frac{E_o}{Z_o} \left[\frac{t^2 e^{-j\beta d}}{1 - \rho^2 e^{-j2\beta d}}\right] \tag{I-12}$$

APPENDIX II

COMPUTER PROGRAM FOR DETERMINING DIELECTRIC CONSTANTS

FORTRAN IV

```
      EXTERNAL FOFE1,FOFE2
      COMMON MAT(1)/BLK1/LAMBDA,S1,D
      LOGICAL TEST
      REAL LAMBDA
      READ(5,2)E1,E2,MAXI,DELTE
    2 FORMAT(2E7.1,I5,F6.3)
   10 WRITE(6,4)
    4 FORMAT(64H1MEASUREMENTS OF DIELECTRIC CONTANT AND LOSS TANGENT A
     1T 60 GHZ/9HOMATERIAL,3X,9HFREQ(GHZ),3X,10HLAMBDA(IN),7X,1HD,10X,2H
     2S1,10X,2HE1,9X,2HA1,7X,4HCODE,7X,2HE2,9X,2HA2,6X,4HCODE)
      DO50J=1,22
      READ(5,1)MAT,FREQ,D,S1,TEST
    1 FORMAT(A6,F10.6,2F8.4,L1)
      IF(TEST)READ(5,5)ALIM,BLIM
    5 FORMAT(2F7.4)
      LAMBDA=3.E+11/(25.4E+9*FREQ)
      CALL ITR2(E5,ALIM,BLIM,DELTE,FOFE1,E1,E2,MAXI,ICODE1)
      DELTE=0.001
      CALL ITR2(E6,ALIM,BLIM,DELTE,FOFE2,E1,E2,MAXI,ICODE2)
      A1=2.*S1*SQRT(E5)/LAMBDA
      A2=2.*S1*SQRT(E6)/LAMBDA
   50 WRITE(6,3)MAT,FREQ,LAMBDA,D,S1,E5,A1,ICODE1,E6,A2,ICODE2
    3 FORMAT(1HO,A6,4X,F10.6,4X,F7.4,3(4X,F8.4),3X,F9.4,5X,I2,4X,F8.4,3X
     1F9.4,4X,I2
      GO TO 10
      END

      FUNCTION FOFE1(EA)
      COMMON/BLK1/LAMBDA,S1,D
      REAL LAMBDA
      TEM=EA
      P=3.1415926/LAMBDA
      TEM1=SIN(P*(S1+D))/COS(P*(S1+D))
      TEM2=SIN(P*S1*SQRT(EA))/(COS(P*S1*SQRT(EA))*SQRT(EA))
      TEM3=TEM1-TEM2
      FOFE1=TEM3
      RETURN
      END
```

```
      FUNCTION FOFE2(EB)
      COMMON/BLK1/LAMBDA,S1,D
      REAL LAMBDA
      P=3.1415926/LAMBDA
      TEM=EB
      TEM1=SIN(P*(S1+D))/COS(P*(S1+D))
      TEM2=SQRT(EB)*SIN(P*S1*SQRT(EB))/COS(P*S1*SQRT(EB))
      TEM3=TEM1-TEM2
      FOFE2=TEM3
      RETURN
      END

$DATA
  .1E-6  .1E-5  200  .001
TEFLON 61.452551  0.0685  1.0221T
 2.0000 4.0000
TEFLON 61.452551  0.0535  1.0221F
TEFLON 61.452551  0.0955  1.0922T
 2.0000 4.0000
TEFLON 61.452551  0.0807  1.0922F
POLSTR 61.452551  0.0290  1.0123T
 2.4000 4.000
POLSTR 61.452551  0.0110  1.0123F
POLSTR 61.452551  0.0485  2.0100T
 2.5000 4.0000
POLSTR 61.452551  0.0255  2.0100F
PLXGLS 61.452551  0.0480  0.3718T
 2.400 4.0000
PLXGLS 61.452551  0.0280  0.3718F
```

SAMPLE OF DATA OBTAINED FROM COMPUTER PROGRAM

MATERIAL	FREQ(GHZ)	LAMBDA(IN)	D	S1	E1	A1	CODE	E2	A2	CODE
TEFLON	61.452551	0.1922	0.0685	1.0221	2.0575	15.2560	0	2.1134	15.4619	0
TEFLON	61.452551	0.1922	0.0535	1.0221	2.0256	15.1375	0	2.0608	15.2682	0
TEFLON	61.452551	0.1922	0.0955	1.0922	2.1006	16.4725	0	2.0481	16.2650	0
TEFLON	61.452551	0.1922	0.0807	1.0922	2.0528	16.2841	0	2.0184	16.1470	0
POLSTR	61.452551	0.1922	0.0290	1.0123	2.5727	16.8962	0	2.5275	16.7471	0
POLSTR	61.452551	0.1922	0.0110	1.0123	2.5329	16.7648	0	2.4568	16.5111	0
POLSTR	61.452551	0.1922	0.0485	2.0100	2.5331	33.2893	0	2.5760	33.5699	0
POLSTR	61.452551	0.1922	0.0255	2.0100	2.5069	33.1164	0	2.5313	33.2776	0
PLXGLS	61.452551	0.1922	0.0480	0.3718	2.8497	6.5311	0	2.6053	6.2449	0
PLXGLS	61.452551	0.1922	0.0280	0.3718	2.6103	6.2508	0	2.4882	6.1029	0

Where:
- Material - dielectric material under test
- Frequency - operating frequency (GHz)
- Lambda - operating wavelength (in.)
- D - shift in plate no. 2 to restore resonance (in.)
- S1 - slab thickness (in.)
- E1 - root satisfying equation (28)
- A1 - ratio $2S_1/\lambda_1$ using E1
- Code - indication whether root exists in prescribed range using equation (28)
- E2 - root satisfying equation (29)
- A2 - ratio $2S_1/\lambda_1$ using E2
- Code - indication whether root exists in prescribed range using equation (29)